MTT Assay

2 10^4 presensitized CBMCs were activated with goat anti-IgE Ab in the presence or absence of IFN- in a total volume of 100 l/well in a 96 well flat-bottomed plate (IWAKI, Tokyo, Japan). 10 l cell count reagent SF (Nakalai, Kyoto, Japan) per well was added after 24 h and MCs were further incubated for 1 h. Optical density values at 450 nm (OD 450) were measured with a microplate reader (BioRad, Hercules, CA).

Flow Cytometric Analysis of OX40L Expression

MCs were presensitized and activated in the presence or absence of 100 ng/ml IFN- . After 24 h, cells were collected and stained with either PE-conjugated anti-human OX40L mAb or PE-conjugated mouse IgG_1 (Becton-Dickinson). After immunofluorescence staining, cells were analyzed with a FACScan flow cytometer (BD Biosciences) using CellQuest software (BD Biosciences).

$CD4^+$ T Cell Proliferation Assay

To avoid the influence of IFN- on $CD4^+$ T cells, MCs that had been presensitized and treated with anti-IgE Ab and IFN- were washed thoroughly and suspended in RPMI1640 supplemented with 10% FBS. Since MCs are unable to proliferate in the absence of SCF, we used MCs without any anti-proliferative treatment such as irradiation and exposure to mitomycin C that might affect the functions of MCs. $CD4^+$ T cells were purified with CD4 isolation kit (Miltenyi Biotech) from PBMC of normal healthy donors. The purity of $CD4^+$ T cells was 95% in all assays performed. In a 96-well round-bottomed plate (IWAKI, Tokyo, Japan), 1 10^5 $CD4^+$ T cells were cultured with 1 10^5 anti-CD3-coated beads (Dynabeads CD3, Dynal Biotech, Oslo, Norway), and activated MCs (at MC/T ratios of 1/5, 1/10, and 1/20) in a total volume of 200 l. To evaluate the involvement of the OX40/OX40L system, some cultures were set up in the presence of either 50 g/ml ik-5 or control IgG2a. Cells were cultured in triplicate for 5 days and pulsed with [^{3}H]thymidine ([^{3}H]TdR) (0.5 Ci/well; MEN Life Science, Boston, MA) for the last 6 h of culture. After harvesting cells, the incorporated radioactivity was measured in a liquid scintillation counter (Packard Instrument Company, Downers Grove, IL).

Statistical Analysis

Statistical analyses were performed by Student's *t*-test or paired *t*-test. Values of p 0.05 were considered to be statistically significant.

RESULTS

TNF- Production was Decreased While IL-10 Production was Increased in IFN- -Treated MCs

MCs are known to release various kinds of cytokines and chemokines upon activation. Among these, TNF- is crucial in MC-$CD4^+$ T interaction (4). IL-10 is an immunoregulatory cytokines which inhibit T cell proliferation. Therefore, we focused on these cytokines and investigated their production in IFN- -treated MCs. Expression of TNF- mRNA was decreased while IL-10 and TGF- mRNA were increased in IFN- -treated MCs (Fig. 1a). To confirm these results, we measured the concentrations of TNF- , IL-10 and TGF- in the supernatants of activated MCs preactivated with or without IFN- by ELISA. As shown in Fig. 1b, pretreatment with IFN- decreased the production of TNF- in a dose-dependent manner. Three independent experiments were done with different CBMC batches to give similar results. The decrease in TNF- production by IFN- (at 100 ng/ml) was statistically significant. Conversely, pretreatment with IFN- increased IL-10 production reproducibly (Fig. 1c). This increase was also statistically significant. TGF- production was slightly increased by IFN- pretreatment, but the difference was not statistically significant (data not shown).

IFN- Treatment did not Affect the Survival of MCs

It is known that the proliferation of human bone marrow-derived MCs was not affected by IFN- treatment (25). However, the effect of IFN- on the survival of CBMC has not been reported. To exclude the possibility that the decrease in cytokine production was due to impaired survival of CBMCs, we performed MTT assay of CBMCs cultured with various concentrations of IFN- . As shown in Fig. 2, IFN- pretreatment did not affect the survival of CBMCs at any concentrations tested.

Pretreatment with IFN- Suppresses OX40L Expression on Activated MCs

OX40 is a costimulatory molecule that potently promotes $CD4^+$ T cell proliferation. Its ligand, OX40L, has been reported to be expressed on human tonsillar and PBMC-derived MCs upon crosslinking of Fc RI and play a vital role in MC-$CD4^+$ T cell interaction although the expression of OX40L on CBMCs has not been reported. In OX40L mice, The severity of EAE was markedly attenuated, whereas it was significantly enhanced in OX40L

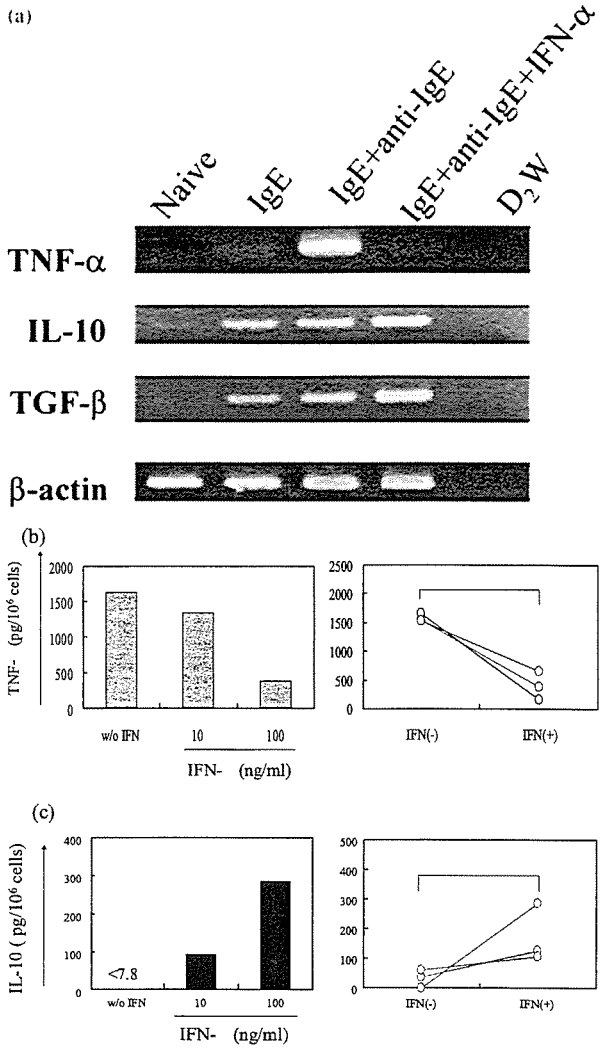

Fig. 1. (a) RT-PCR for TNF- , IL-10, and TGF- . PCR products were electrophoresed on 1.5% agarose gel. Data shows a representative of three independent experiments. (b) and (c) ELISA assay of TNF- and IL-10. TNF- and IL-10 productions of presensitized CBMCs activated in the presence or absence of IFN- were measured by ELISA. A representative of three independent experiments for each cytokine is shown (left). The difference in each cytokine production (pg/ml) between the absence and presence of 100 ng/ml IFN- was analyzed statistically. p 0.05.

transgenic mice (26). If MCs participate in the pathogenesis of EAE, it is likely that OX40L expressed on MCs are involved in such process. We first confirmed that OX40L was also expressed on CBMCs after Fc RI crosslinking as reported with tonsillar and PBMC-derived MCs and found that pretreatment with IFN- considerably suppressed its expression (Fig. 3).

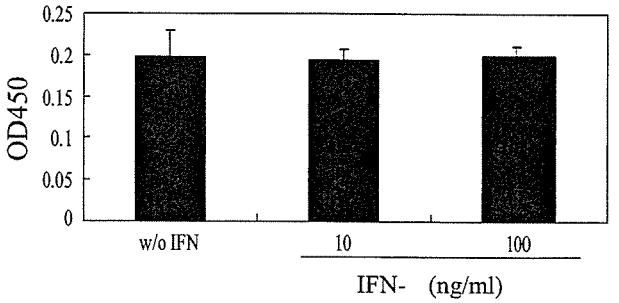

Fig. 2. Survival of IFN- -treated MCs was measured by MTT assay. MTT assay was performed 24 h after activation with anti-IgE Ab and the indicated concentrations of IFN- . Data indicate mean ± SD of triplicate wells of a representative of three independent experiments.

Pretreatment of MCs with IFN- Significantly Inhibited Costimulation of CD4⁺ T Cells by CBMCsn

Finally we examined the effects of IFN- on T cell activating functions of MCs, because TNF- and OX40L which we showed were suppressed by IFN- are both important factors for T cell costimulation by MCs. We cocultured $CD4^+$ T cells from normal healthy donors and preactivated MCs with or without IFN- treatment, and analyzed T cell proliferation on day 5. In this assay, IFN- and anti-IgE Ab were washed out before coculture in order to exclude the effect of IFN- on $CD4^+$ T cells. As shown in Fig. 4a, IFN- -treated MCs induced lower levels of T cell proliferation compared with non-treated MCs, indicating that IFN- suppressed T cell activating functions of MCs. The OX40/OX40L system is reported to play a role in MC-T cell interaction in humans (8). In accordance with the previous report, an addition of anti-OX40L mAb significantly suppressed the costimulatory functions of activated CBMCs (Table I).

DISCUSSION

Accumulating evidence has indicated that MCs are not simple effector cells in allergic reactions but are multifunctional accessory cells for T cell responses that influence the magnitude and direction of adaptive immunity. Consistent with this new concept, MCs have been shown to play important roles in the pathogenesis of not only Th2 diseases but also some Th1 diseases such as inflammatory bowel disease and MS (11, 12). Thus, it is essential to understand the regulation of MC functions in order to elucidate the MC-mediated pathogenesis and control of the diseases.

In the present study, we showed that pretreatment of MCs with IFN- decreased TNF- production and

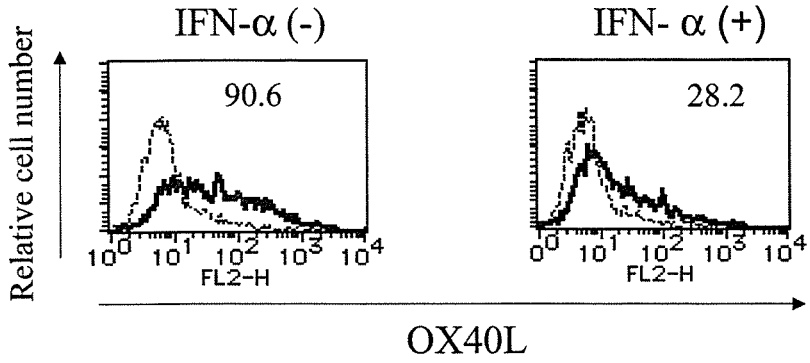

Fig. 3. OX40L expression on activated CBMCs. Presensitized MCs activated in the absence or presence of 100 ng/ml IFN- were subjected to flow cytometric analysis. Data of a representative of three independent experiments are shown. Numbers in the histograms indicate MFI of OX40L expression.

OX40L expression, while IL-10 production was increased. In accordance with these results, IFN- significantly suppressed the costimulatory functions of MCs in coculture with $CD4^+$ T cells. In the literature, we found two primitive reports that IFN- / plus IFN- suppressed TNF- mRNA levels in rat MC lines and rat peritoneal MCs (27), and that in vivo topical administration of IFN- to nasal mucosa of allergic patients resulted in an decrease in TNF- $^+$ mucosal MC number in the biopsy specimens (28). In these reports, however, the effects of type I IFNs on actual TNF- secretion, on other cytokine productions, on OX40L expression, or on T cell costimulatory functions were not investigated. Thus, the effects of IFN- on MC functions have never been studied in detail. As far as we know, the present study is the first to delineate the entire picture of the effects of IFN- on the MC functions.

IFN- -induced increase in IL-10 production by MCs is particularly important because IL-10 negatively affects immune responses by inhibiting the production of inflammatory cytokines. IL-10 is reported to suppress the release of inflammatory cytokine by MCs in an autocrine manner (20). Thus, it is possible that inhibition of TNF- production presented in this study was mediated by increased IL-10 that was induced by IFN- treatment. In allergic reactions, the role of IL-10-secreting T(R)1 cells is reported to induce tolerance (29). However, the role of IL-10 secreted by MCs in the context of adaptive immunity has never been reported. Our results suggest the possibility that immunoregulatory cytokines derived from IFN- -treated MCs may contribute to the suppression of costimulatory function of MCs themselves and other surrounding immune cells leading to regulation of the overall inflammatory reactions.

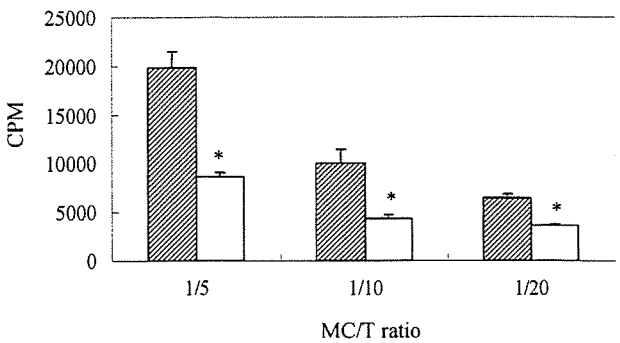

Fig. 4. Coculture of CBMCs and $CD4^+$ T from normal healthy donors. Presensitized CBMCs were activated with goat anti-IgE in the presence or absence of 100 ng/ml IFN- for 24 h and subsequently washed. 1 10^5 T cells were cocultured with MCs at indicated MC/T ratios in the presence of anti-CD3-coated beads for 5 days. Cells were pulsed with [^{3}H]TdR for the last 6 h of culture and the incorporated radioactivity was measured by a liquid scintillation counter. Data indicate mean ± SD of triplicate wells. Striped bars indicate CBMCs activated without IFN- and white bars indicate CBMCs activated with IFN- . p 0.05 compared with "without IFN- ."

Table I. The Effect of Anti-OX40L mAb on the Costimulatory Activities of CBMCs

	CPM ± SD
w/o mAb	10118 ± 1303
Control	13047 ± 490
ik-5	7132 ± 350

Notes. Presensitized CBMCs were activated with IgE and anti-IgE Ab, washed, and then cocultured with $CD4^+$ T cells and anti-CD3-coated beads in the absence or presence of either 50 g/ml ik-5 or control IgG2a for 5 days. T cell proliferation was measured by [^{3}H]TdR incorporation for the last 6 h. Three independent experiments were done and gave similar results. Data indicate the mean ± SD of triplicate cultures of a representative experiment.

Downregulation of OX40L expression on MCs by IFN- is also impressive. OX40L can be induced on human peripheral blood stem cells-derived MCs in vitro and human MCs isolated from tonsil and lung (8). These MCs have been reported to interact directly with $CD4^+$ T cells and augment their proliferation mainly via the OX40/OX40L system. It is now recognized that expression of OX40L on antigen presenting cells that stand for mostly dendritic cells (DCs) is the key event for promotion of inflammatory responses. In fact, OX40/OX40L system is implicated in the exacerbation of EAE (26, 30). Considering that presence of MCs is required for the development of severe EAE, it is possible that type I IFNs ameliorate the manifestations of MS by suppressing the expression of OX40L on MCs.

In conclusion, we showed here that type I IFNs attenuate T cell activating functions of human MCs by decreasing TNF- production and OX40 ligand expression while increasing IL-10 production. Effectiveness of type I IFNs in the treatment of MS is still an enigma, since IFNs are considered to be a proinflammatory cytokine enhancing Th1 immune responses. The present study provides a novel insight into the inhibitory aspects of IFNs action and presents the possibility that IFNs might influence T cell response via their regulatory effects on MCs in inflammatory Th1 diseases including MS.

ACKNOWLEDGMENTS

This work was partly supported by grants-in-aid from the Ministry of Health, Labour and Welfare of Japan.

REFERENCES

1. Galli SJ: Mast cells and basophils. Curr Opin Hematol 7:32–39, 2000
2. Kawakami T, Galli SJ: Regulation of mast-cell and basophil function and survival by IgE. Nat Rev Immunol 2:773–786, 2002
3. McLachlan JB, Hart JP, Pizzo SV, Shelburne CP, Staats HF, Gunn MD, Abraham SN: Mast cell-derived tumor necrosis factor induces hypertrophy of draining lymph nodes during infection. Nat Immunol 4:1199–1205, 2003
4. Nakae S, Suto H, Kakurai M, Sedgwick JD, Tsai M, Galli SJ: Mast cells enhance T cell activation: Importance of mast cell-derived TNF. Proc Natl Acad Sci USA 102:6467–6472, 2005
5. Frandji P, Mourad W, Tkaczyk C, Singer M, David B, Colle JH, *et al.*: IL-4 mRNA transcription is induced in mouse bone marrow-derived mast cells through an MHC class II-dependent signaling pathway. Eur J Immunol 28:844–854, 1998
6. Frandji P, Oskeritzian C, Cacaraci F, Lapeyre J, Peronet R, David B, *et al.*: Antigen-dependent stimulation by bone marrow-derived mast cells of MHC class II-restricted T cell hybridoma. J Immunol 151:6318–6328, 1993
7. Skokos D, Le Panse S, Villa I, Rousselle JC, Peronet R, David B, *et al.*: Mast cell-dependent B and T lymphocyte activation is mediated by the secretion of immunologically active exosomes. J Immunol 166:868–876, 2001
8. Kashiwakura J, Yokoi H, Saito H, Okayama Y: T cell proliferation by direct cross-talk between OX40 ligand on human mast cells and OX40 on human T cells: Comparison of gene expression profiles between human tonsillar and lung-cultured mast cells. J Immunol 173:5247–5257, 2004
9. Nakae S, Suto H, Iikura M, Kakurai M, Sedgwick JD, Tsai M, *et al.*: Mast cells enhance T cell activation: importance of mast cell costimulatory molecules and secreted TNF. J Immunol 176:2238–2248, 2006
10. Pawankar R: Mast cells in allergic airway disease and chronic rhinosinusitis. Chem Immunol Allergy 87:111–129, 2005
11. Araki Y, Andoh A, Fujiyama Y, Bamba T: Development of dextran sulphate sodium-induced experimental colitis is suppressed in genetically mast cell-deficient Ws/Ws rats. Clin Exp Immunol 119:264–269, 2000
12. Skaper SD, Facci L, Romanello S, Leon A: Mast cell activation causes delayed neurodegeneration in mixed hippocampal cultures via the nitric oxide pathway. J Neurochem 66:1157–1166, 1996
13. Secor VH, Secor WE, Gutekunst CA, Brown MA: Mast cells are essential for early onset and severe disease in a murine model of multiple sclerosis. J Exp Med 191:813–822, 2000
14. Olsson Y: Mast cells in plaques of multiple sclerosis. Acta Neurol Scand 50:611–618, 1974
15. Tuomisto L, Kilpelainen H, Riekkinen P: Histamine and histamine-*N*-methyltransferase in the CSF of patients with multiple sclerosis. Agents Actions 13:255–257, 1983
16. Rozniecki JJ, Hauser SL, Stein M, Lincoln R, Theoharides TC: Elevated mast cell tryptase in cerebrospinal fluid of multiple sclerosis patients. Ann Neurol 37:63–66, 1995
17. Virley DJ: Developing therapeutics for the treatment of multiple sclerosis. NeuroRx 2:638–649, 2005
18. Berghella AM, Totaro R, Pellegrini P, Contasta I, Russo T, Carolei A, *et al.*: Immunological study of IFNbeta-1a-treated and untreated multiple sclerosis patients: clarifying IFNbeta mechanisms and establishing specific dendritic cell immunotherapy. Neuroimmunomodulation 12:29–44, 2005
19. Imura A, Hori T, Imada K, Ishikawa T, Tanaka Y, Maeda M, *et al.*: The human OX40/gp34 system directly mediates adhesion of activated T cells to vascular endothelial cells. J Exp Med 183:2185–2195, 1996
20. Royer B, Varadaradjalou S, Saas P, Gabiot AC, Kantelip B, Feger F, *et al.*: Autocrine regulation of cord blood-derived human mast cell activation by IL-10. J Allergy Clin Immunol 108:80–86, 2001
21. Carre PC, Mortenson RL, King TE, Jr., Noble PW, Sable CL, Riches DW: Increased expression of the interleukin-8 gene by alveolar macrophages in idiopathic pulmonary fibrosis. A potential mechanism for the recruitment and activation of neutrophils in lung fibrosis. J Clin Invest 88:1802–1810, 1991
22. Li DQ, Luo L, Chen Z, Kim HS, Song XJ, Pflugfelder SC: JNK and ERK MAP kinases mediate induction of IL-1beta, TNF-alpha and IL-8 following hyperosmolar stress in human limbal epithelial cells. Exp Eye Res 82:588–596, 2006
23. de Saint-Vis B, Fugier-Vivier I, Massacrier C, Gaillard C, Vanbervliet B, Ait-Yahia S, *et al.*: The cytokine profile expressed

by human dendritic cells is dependent on cell subtype and mode of activation. J Immunol 160:1666–1676, 1998
24. Diamond MP, El-Hammady E, Wang R, Saed G: Regulation of transforming growth factor-beta, type III collagen, and fibronectin by dichloroacetic acid in human fibroblasts from normal peritoneum and adhesions. Fertil Steril 79:1161–1167, 2003
25. Kirshenbaum AS, Worobec AS, Davis TA, Goff JP, Semere T, Metcalfe DD: Inhibition of human mast cell growth and differentiation by interferon gamma-1b. Exp Hematol 26:245–251, 1998
26. Ndhlovu LC, Ishii N, Murata K, Sato T, Sugamura K: Critical involvement of OX40 ligand signals in the T cell priming events during experimental autoimmune encephalomyelitis. J Immunol 167:2991–2999, 2001
27. Bissonnette EY, Chin B, Befus AD: Interferons differentially regulate histamine and TNF-alpha in rat intestinal mucosal mast cells. Immunology 86:12–17, 1995
28. Riccardi-Arbi R, Bacci S, Romagnoli P, Rucci L: Interferon-alpha affects the tumour necrosis factor-alpha content of mast cells in human nasal mucosa. A pilot study in allergic patients. Ital J Anat Embryol 109:115–122, 2004
29. Akdis M, Blaser K, Akdis CA: T regulatory cells in allergy. Chem Immunol Allergy 91:159–173, 2006
30. Carboni S, Aboul-Enein F, Waltzinger C, Killeen N, Lassmann H, Pena-Rossi C: CD134 plays a crucial role in the pathogenesis of EAE and is upregulated in the CNS of patients with multiple sclerosis. J Neuroimmunol 145:1–11, 2003

Review Article

Nucleophosmin: A versatile molecule associated with hematological malignancies

Tomoki Naoe,[1,4] Tatsuya Suzuki,[1] Hitoshi Kiyoi[2] and Takeshi Urano[3]

Departments of [1]Hematology and Oncology, [2]Infectious Diseases, and [3]Biochemistry, Nagoya University Graduate School of Medicine, Tsurumai-cho 65, Showa-ku, Nagoya 466-8550, Japan

(Received May 10, 2006/Accepted May 29, 2006/Online publication July 27, 2006)

Nucleophosmin (NPM) is a nucleolar phosphoprotein that plays multiple roles in ribosome assembly and transport, cytoplasmic-nuclear trafficking, centrosome duplication and regulation of p53. In hematological malignancies, the *NPM1* gene is frequently involved in chromosomal translocation, mutation and deletion. The *NPM1* gene on 5q35 is translocated with the anaplastic lymphoma kinase (*ALK*) gene in anaplastic large cell lymphoma with t(2;5). The *MLF1* and *RARA* genes are fused with *NPM1* in myelodysplastic syndrome and acute myeloid leukemia (AML) with t(3;5) and acute promyelocytic leukemia with t(5;17), respectively. In each fused protein, the N-terminal NPM portion is associated with oligomerization of a partner protein leading to altered signal transduction or transcription. Recently, mutations of exon 12 have been found in a significant proportion of *de novo* AML, especially in those with a normal karyotype. Mutant NPM is localized aberrantly in the cytoplasm, but the molecular mechanisms for leukemia remain to be studied. Studies of knock-out mice have revealed new aspects regarding *NPM1* as a tumor-suppressor gene. This review focuses on the clinical significance of the *NPM1* gene in hematological malignancies and newly discovered roles of NPM associated with oncogenesis. (*Cancer Sci* 2006; 97: 963–969)

Nucleophosmin (NPM), also called B23, numatrin or NO38, was isolated as an abundant nucleolar phosphoprotein, whose expression level is increased significantly by several kinds of stimulation and transformation.[1,2] In 1989, a human NPM cDNA encoding a 294-amino-acid protein was cloned.[3] In 2002, a shorter isoform encoding a 259-amino acid protein that differs at the C-terminus was also isolated.[4] The *NPM1* gene spans 25 kb, contains 12 exons and maps to chromosome 5q35.[4,5] Exon 8 is frequently skipped, and exon 10 is used only for the short isoform. Although the biological significance of the short isoform remains unclear, its expression is increased in radiation-insensitive cell lines and the product is localized in the cytoplasm as well as in the nucleus.[4,6] The structural features of NPM consist of an oligomerization domain, a metal-binding motif, a bipartite nuclear localization signal, two Asp/Glu-rich domains, phosphorylation sites for CDK2 and a nucleor localization signal.[6,7]

NPM1 has been recognized by oncologists as a partner gene for various chromosomal translocations: *NPM*–anaplastic lymphoma kinase (*ALK*) in anaplastic large cell lymphoma (ALCL) with t(3;5), *NPM–RARA* in acute promyelocytic leukemia (APL) with t(5;17), and *NPM–MLF1* in acute myeloid leukemia (AML)/myelodysplastic syndrome (MDS) with t(3;5).[8–10] (Fig. 1, 2) In each chimeric gene product, the N-terminal NPM portion is thought to act as the interface for oligomerization and oncogenic conversion of the C-terminal functional domain such as a kinase or transcription factor. Recently, NPM was associated with centrosome duplication and the regulation of p53,[11,12] and might have a role as a tumor suppressor.

Expression and function of NPM

Nucleophosmin is an abundant and ubiquitously expressed phosphoprotein. It is located mainly in the nucleolus and shuttles between the nucleus and cytoplasm.[13,14] NPM has been proposed to be associated with the synthesis and processing of ribosomal RNA (rRNA), regulation of chromatin structure and transport of rRNA and ribosomal proteins.[15,16] However, a recent study using knock-out mice suggests that NPM is not indispensable for these biological processes, as shown below.

The NPM level is increased in proliferating cells as well as tumor cells, perhaps due to an increased requirement for ribosomal synthesis. Overexpression or downregulation of NPM reportedly alters the cellular status with respect to proliferation, differentiation and apoptosis, although some contradictory results have been reported.[17,18] NPM function appears to be different depending on whether or not wild-type p53 is present.[12,19]

It has been reported that NPM has an important role in the cell cycle. NPM interacts with the centrosome and protects it from duplication in G_1 phase.[20] It is expressed highly during S and G_2 phases and is duplicated concomitantly with the initiation of DNA synthesis. Okuda *et al.* reported that the temporal activation of cyclin-dependent kinase (CDK)/cyclin E, which is associated with DNA replication–initiation factors, occurs simultaneously with phosphorylation of NPM, which occurs initially in centrosome duplication.[21,22] Phosphorylated NPM leaves the centrosomes during their duplication. Dissociation of NPM from the centrosome allows the centrosome duplication process during S phase. NPM was reported to reassociate with the centrosome in mitosis. Cha *et al.* reported that CDK1/cyclin B, a key regulator of M phase, phosphorylates another site of NPM and allows NPM to target to the centrosome during mitosis.[23]

Regarding the anti-oncogenic role of NPM, it is notable that NPM binds to p53 and its associated proteins. NPM has been implicated in the acute response of mammalian cells to various DNA-damaging stresses, such as radiation and ultraviolet (UV) light.[24] The stability of p53 is regulated primarily by MDM2, which is a ubiquitin E3 ligase.[25] MDM2 is regulated negatively by Arf, which binds to MDM2 and promotes its rapid degradation. NPM has been reported to form a molecular complex consisting of p53, MDM2 and Arf.[26,27]

Colombo *et al.* reported that NPM interacts directly with p53, increases its stability and activates the transcriptional function of p53 after DNA-damaging stress, and induces p53-dependent premature senescence in mouse embryonic fibroblasts.[12] Kurki *et al.* demonstrated that NPM activated by UV or viral stress is redistributed to the nucleoplasm, binds to MDM2, and leads to

[4]To whom correspondence should be addressed. E-mail: tnaoe@med.nagoya-u.ac.jp

doi: 10.1111/j.1349-7006.2006.00270.x

the stabilization of p53.[19] However, although Arf is a nucleolar protein that binds and inactivates MDM2 in the nucleoplasm, Korgaonkar *et al.* showed that Arf functions primarily outside the nucleolus, and it is sequestered and held inactive in the compartment by NPM.[28] Most likely, NPM inhibits Arf's p53-dependent activity by targeting it to nucleoli and impairing ARF–MDM2 association.

In accordance with these findings, knock-out (KO) mice of the *NPM1* gene show mid-stage embryonic lethality due to the accumulation of DNA damage, activation of p53, and widespread apoptosis.[29,30] Double KO mice of *TP53* and *NPM1* rescue apoptosis *in vivo* and fibroblast proliferation *in vitro*.[29] In the absence of NPM, Arf protein is excluded from nucleoli and is markedly less stable. It has been suggested that NPM regulates DNA integrity through Arf–MDM2–p53.

Conversely, it was also shown that Arf inhibits the production of rRNA, retarding the processing of 47/45S and 32S precursors.[31] Itahana *et al.* further reported that Arf promotes polyubiquitination and degradation of NPM.[32] Accordingly, there is a molecular association between NPM and Arf, which implies a new role for the nucleolus in oncogenesis.

NPM–ALK chimeric kinase in ALCL

Anaplastic large cell lymphoma is a T-cell lymphoma that is characterized by abundant cytoplasm, pleomorphic nuclei and CD30 expression.[33] ALCL accounts for approximately 3% of adult non-Hodgkin's lymphoma and 10–30% of childhood lymphoma. Cytogenetically, the 2p23 locus is translocated frequently with 5q35, and less frequently with 1p25, 3q21 or 2q35.[34] In 1994, Morris *et al.* showed that the t(2;5) translocation fused the *NPM1* gene on 5q35 to a previously unidentified protein tyrosine kinase gene, *ALK*, on 2p23.[35]

In the NPM–ALK chimeric kinase, the N-terminus of NPM (amino acids 1–117) is fused to the catalytic domain of ALK (amino acids 1058–1620). Because its expression is regulated by the *NPM1* promoter, the fusion protein is expressed ectopically in lymphoid tissue. Wild-type ALK is a receptor tyrosine kinase that is expressed in the brain, spinal cord, small intestine and testis, but not in lymphoid cells. ALK belongs to the insulin receptor subfamily, although the natural ligand remains unclear.[36] In NPM–ALK, the N-terminal NPM domain is associated with oligomerization (Fig. 3) and causes constitutive activation of the ALK kinase. This mechanism is similar to that of BCR–ABL. NPM–ALK can associate with several adaptor proteins such as SHC, Grb2 and IRS-1, and is associated with the activated RAS–MAPK, PLCg, PI3K–Akt and JAK–STAT pathways.[34,37–39] Experiments using Ba/F3 cells revealed that NPM–ALK abrogates the interleukin-3 dependency of the cells and mediates signals for proliferation and survival.

Because NPM–ALK$^+$ lymphomas express CD30, a transmembrane receptor for CD30L, it has been asked whether CD30 and NPM–ALK are connected functionally.[40] In Hodgkin's lymphoma, overexpressed CD30 molecules aggregate on the cell surface ligand-independently, and form a TRAF–IKK–IKBα complex, which leads to nuclear factor kappa-B (NF-κB) activation.[41] In contrast, Horie *et al.* clarified that NPM–ALK disrupts CD30 signaling and constitutive NF-κB activation in ALCL.[42] TRAF2/5 was shown to be bound with NPM–ALK on both the kinase domain of ALK and the N-terminal domain of NPM. In the same study, wild-type NPM was shown to be tyrosine-phosphorylated by NPM–ALK, although the significance remains unclear.

Studies of subcellular localization of NPM and its chimeric proteins reveal another aspect of the oncogenic role of NPM.[43] As shown in Fig. 1, NPM–ALK consists structurally of the oligomerization and metal-binding domains of NPM together with an almost full-sized intracytoplasmic domain of ALK. It lacks the two nuclear localization domains and Asp/Glu-rich domains

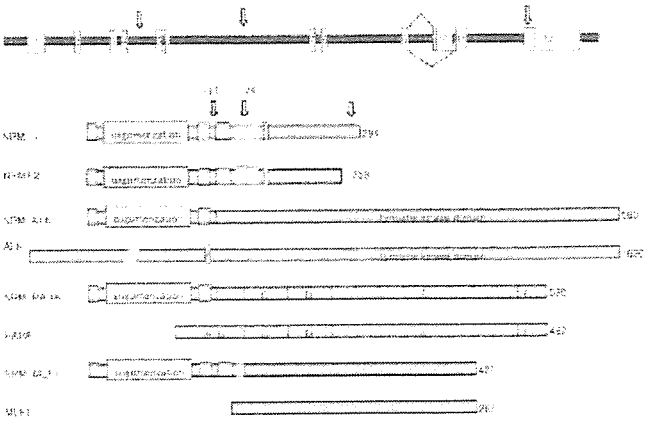

Fig. 1. The *NPM1* gene and its related cDNA. Two isoforms of *NPM1* cDNA differ at the C-terminus. Exon 9 is spliced with exon 11 in *NPM1.1*, whereas in *NPM1.2* it is spliced with exon 10 and the coding sequence is terminated prematurely. In nucleophosmin (NPM)–ALK, the cytoplasmic domain of ALK is fused with the N-terminal NPM domain, which contains an oligomerization domain. Similar to NPM–ALK, the entire functional domain of RARA is fused to the N-terminal NPM domain, which accelerates oligomerization and inactivation of retinoic acid-responsive transcription. Break points are indicated by yellow arrows. The clustering regions of mutations of exon 12 are indicated by a red arrow.

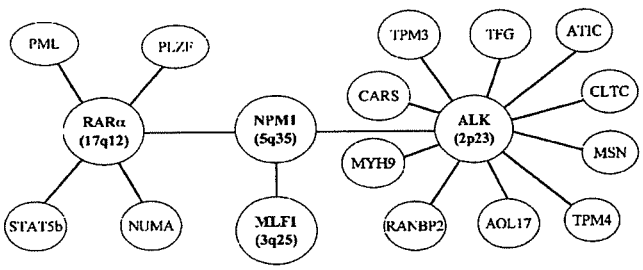

Fig. 2. Fusion genes with the *NPM1* gene.

of NPM. Accordingly, NPM–ALK is thought to be localized to the cytoplasm instead of nucleoli. Immunohistochemistry using anti-ALK stains both the nucleus and cytoplasm of ALCL cells[36,43,44] (Fig. 4). Anti-C-terminal NPM antibody is able to discriminate wild-type NPM from the fused protein. Interestingly, wild-type NPM is localized to the nucleus but not the cytoplasm, whereas NPM–ALK is distributed in both.

There are many *in vivo* studies on the oncogenic role of NPM–ALK.[39] Mice transplanted with bone marrow cells infected with retrovirus containing human *NPM1–ALK* cDNA developed B-cell lymphoma, not ALCL. However, in transgenic mice carrying *NPM1–ALK* cDNA under the control of the murine CD4 promoter or Moloney murine leukemia virus Long Terminal Repeat (LTR), T-cell tumors resembling human ALCL developed, suggesting that the phenotype depends on the promoter.

NPM–RARα chimeric transcription factor in APL

Acute promyelocytic leukemia is characterized by myeloid malignancies with a maturational block at the promyelocytic stage.[33] Treatment with all-*trans* retinoic acid (ATRA) overcomes this maturation arrest and induces differentiation of APL blasts.[45] APL is usually accompanied by t(15;17), which

doi: 10.1111/j.1349-7006.2006.00270.x

Fig. 3. The structure of the N-terminal domain of *Xenopus* nucleoplasmin (Np-core), which is related to NPM1, was reported by Namboodiri *et al.*[73] The Np-core monomer forms a barrel shape consisting of eight-stranded β-sheets, and the barrel forms a stable pentamer. Two pentamers further associate to form a decamer. The authors showed that both Np and Np-core are able to assemble large complexes that contain the four core histones. These complexes each contain five histone octamers that dock to a central Np decamer. Dutta *et al.* provided models of histone storage, sperm chromatin decondensation and nucleosome assembly.[15]

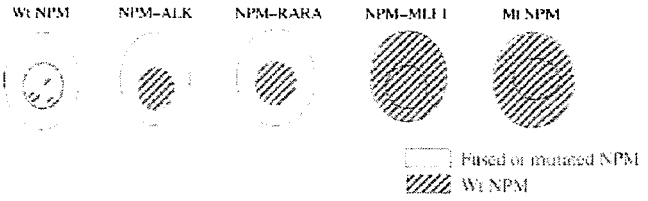

Fig. 4. Subcellular localization of nucleophosmin (NPM) and its fused proteins. The distribution of NPM–ALK homodimer is limited to the cytoplasm, but the nucleolar localization motifs present in wild-type (Wt) NPM permits entry of the NPM/NPM–anaplastic lymphoma kinase (ALK) heterodimers to the nucleus and nucleolus.[36] Although data of the localization of NPM–RARα is limited, transfection of *NPM1–RARA* into Hela cells showed a diffuse pattern of nuclear localization.[57] In contrast, NPM–MLF1 and wild-type NPM were stained by using anti-C-terminal NPM antibody.[60]

forms the *PML–RARA* fusion gene.[46] In addition, molecular variants of APL have been described in which *RARA* is fused to one of four other genes: *PLZF*, *NUMA*, *STAT5b* or *NPM1*.[46,47] Common features of all of these proteins are that the B through F regions of RARα, which contain its DNA and ligand-binding domains, have N-terminal non-RARα moieties that add dimerization ability to each fusion protein. Homodimerization or heterodimerization is thought to be associated with the repression of retinoid-responsive transcription and perhaps with other alterations in transcription.

The first APL case with a t(5;17) translocation was described in 1994 and the sequence of chromosomal joint was cloned in 1996.[48,49] This variant type of APL was clinically sensitive to ATRA, and the sensitivity was later confirmed *in vitro*.[50] The N-terminal NPM portion fuses with RARα in a similar manner to other APL fusion products. Like other APL fusion products, NPM–RARα forms a heterodimer with RXR or NPM. These dimers recruit corepressor complexes and repress retinoid-responsive transcription in a dominant-negative manner.[51] Homodimer formation of RARα may be a crucial event in APL pathogenesis *in vivo*.[52] In transgenic mice, NPM–RARα enhanced the proliferation of myeloid cells, mimicking myeloproliferative disease and, later, the transgenic mice developed an APL-like disease with blasts that were sensitive to ATRA.[53]

In the case of PML–RARα, immunostaining with anti-PML antibody revealed a microgranular pattern, which differs from the microspeckled one observed in the case of wild-type PML.[54] ATRA treatment restored the aberrant localization to a speckled pattern through degradation of PML–RARα.[55,56] This finding implies that NPM–RARα also acts in a dominant-negative manner relative to wild-type PML, and this effect is cancelled by ATRA. Anti-NPM (N-terminus) antibody stained the nucleus with a diffuse microgranular pattern, whereas PML localization was normal.[57] It is interesting but remains to be studied how NPM–RARα affects the function of wild-type NPM.

NPM–MLF1 chimeric protein in AML/MDS

Yoneda-Kato *et al.* reported that the t(3,5) (q25.1;q34) translocation associated with AML/MDS (most frequently with the M6 French–American–British [FAB]-type) produces a 5′-NPM-coding sequence fused in-frame to a new gene, which they named *MLF1*.[10] The *MLF1* gene encodes a 268-amino-acid polypeptide that has no homology to any previously characterized protein and does not have known functional motifs. Expression of *MLF1* mRNA is observed in testis, ovary, skeletal muscle, heart, kidney and colon, but not in normal hematopoietic cells.

The function of MLF1 protein remains unclear, but it inhibits erythropoietin-induced differentiation, cell-cycle exit and p27KIP1 accumulation.[58] Hanissian *et al.* identified an MLF1-interacting protein (MLF1IP) that associates specifically with MLF1. MLF1IP has nuclear localization signals, two nuclear receptor-binding motifs (LXXLL), two leucine zippers, two polypeptide enriched in proline, glutamine, serine and threonine (PEST) residues and several potential phosphorylation sites.[59] MLF1IP seems to have an important role in erythroid differentiation, and MLF1 seems to regulate MLF1IP function negatively.

Immunostaining studies have shown that MLF1 is localized mainly in the cytoplasm, whereas the NPM–MLF1 fusion protein is localized in the nucleus, especially the nucleolus[60] (Fig. 4). NPM is a nuclear protein and therefore the N-terminal portion that is fused to MLF1 may carry the nuclear targeting signal. Thus, both the ectopic expression and aberrant subcellular localization of MLF1 seem to be associated with the interruption of erythroid differentiation, which may be the reason that *MPL–MLF1* is found entirely in M6 FAB-type AML/MDS.

Frameshift mutation of NPM1 in AML

During an extensive study of the subcellular localization of NPM, Falini *et al.* found a correlation between the presence of cytoplasmic NPM and clinical and biological features in AML samples.[61] Cytoplasmic NPM was detected in 35.2% of 591 bone marrow specimens from patients with primary AML but not in 135 secondary AML specimens or in 980 hematopoietic or non-hematopoietic neoplasms other than AML. It was associated with a wide spectrum of morphological subtypes of the disease from M0 to M7 except M3. A normal karyotype and responsiveness to induction chemotherapy were also related to cytoplasmic NPM. There was a high frequency of internal tandem duplications of FLT3 (FLT3/ITD) and lack of CD34 and CD133 expression. AML with cytoplasmic NPM carried novel mutations in exon 12 of the *NPM1* gene. In the most common mutation, called type A, a 4-bp nucleotide (TCTG) is inserted at the position encoding the 288th amino acid residue, causing a frameshift of the downstream coding sequence (Table 1). As a result, the C-terminal amino acid residues, 286DLWQWRKSL-COOH, are changed to 286DLCLAVEEVSLRK-COOH. So far, a total of 29 variant sequence mutations have been reported in the *NPM1* genes of 1557 patients. All of the NPM mutant proteins lose at least one of W288 and W290, and share the same last five amino

Table 1. Representative mutations of *NPM1* in AML

Mutation	Sequence	Predicted amino-acid
Wild type (*NPM1.1*)	GAT CTC TGG CAG TGG AGG AAG TCT CTT **TAA** GAAAATAG	-DLWQWRKSL
Mutation A	GAT CTC TGT CTG GCA GTG GAG GAA GTC TCT TTA AGA AAA TAG	-DLCLAVEEVSLRK
Mutation B	GAT CTC TGC ATG GCA GTG GAG GAA GTC TCT TTA AGA AAA TAG	-DLCMAVEEVSLRK
Mutation D	GAT CTC TGC CTG GCA GTG GAG GAA GTC TCT TTA AGA AAA TAG	-DLCLAVEEVSLRK

The four inserted nucleotides are underlined. Stop codon is in bold. The nucleolar localization signal WXW in the wild-type sequence is substituted by LXXXVXXVXL, which corresponds to a nuclear export signal, shown in the predicted amino-acid column.

acid residues (VSLRK). Thus, despite the genetic heterogeneity, all of these *NPM1* gene mutations have the common feature of a frameshift mutation at the C-terminal region. Nakagawa *et al.* noticed that this frameshift not only loses the nucleolar localization signal (WXW) but also gains a nuclear export signal (NES) consisting of LXXXVXXVXL.[62] Falini *et al.* further confirmed that both alterations are crucial for NPM mutant export from the nucleus to the cytoplasm.[63]

Falini *et al.* found that cytoplasmic staining of NPM could define the *NPM1* mutation-positive AML cases that had a normal karyotype, *NPM1* gene mutations, and responsiveness to induction chemotherapy.[61] Grisendi and Pandolfi noted that NPM staining in cases of AML with aberrant cytoplasmic localization of the protein is mostly cytoplasmic, which suggests that the mutant NPM acts predominantly on the product of the remaining wild-type allele, causing its retention in the cytoplasm by heterodimerization[64] (Fig. 4).

Based on the above report, Suzuki *et al.* identified similar *NPM1* mutations, including four novel sequence variants, in 64 of 257 (24.9%) Japanese patients with *de novo* AML.[65] *NPM1* mutations were associated with normal karyotypes and with *FLT3* mutations, but not with other mutations. In 190 patients without the M3 FAB subtype who were treated using the protocol of the Japan Adult Leukemia Study Group, multivariate analyses showed that the *NPM1* mutation was a favorable factor for achieving complete remission but was associated with a high relapse rate. Importantly, sequential analysis using 39 paired samples obtained at diagnosis and relapse showed that *NPM1* mutations were lost at relapse in two of the 17 patients who had *NPM1* mutations at diagnosis. The loss of *NPM1* mutation at relapse suggests that it is not necessarily needed for maintenance of the disease.

Schnittger *et al.* screened 401 AML patients with normal karyotypes treated using the German AML Cooperative Group Protocol 99 for *NPM1* mutations.[66] *NPM1* mutations were detected in 212 (52.9%) of the 401 patients. Fourteen mutations, including eight new variants, were identified. *NPM1*-mutated cases were frequently associated with *FLT3* mutations but rarely associated with *MLL* tandem duplication, *NRAS*, *KIT* and *CEBPA* mutations. The *NPM1*-mutated group had a higher complete remission (CR) rate, a tendency of longer overall survival (OS), and significantly longer event-free survival (EFS).

Roel *et al.* examined *NPM1* mutation status in a cohort of 275 patients with AML by denaturing high-performance liquid chromatography.[67] *NPM1* mutations are less frequent in younger patients than in those aged over 35 years. *NPM1* mutations are positively correlated with AML with high white blood cell counts, normal karyotypes, and *FLT3/ITD*. *NPM1* mutations are correlated inversely with the occurrence of *CEBPA* and *NRAS* mutations. AML patients with *NPM1* mutations have a significantly better OS and EFS than those without *NPM1* mutations. Finally, in multivariate analysis, *NPM1* mutations have an independent favorable prognostic value with regard to OS, EFS and DFS.

In 300 patients entered into the AML Study Group trials, *NPM1* mutations were identified in 48% of the patients, including 12 novel sequence variants, all leading to a frameshift in the C-terminus of NPM.[68] AML patients with *NPM1* mutations in the absence of *FLT3/ITD* define a distinct molecular and prognostic subclass of young adult AML patients with normal cytogenetics.

In a larger study, the clinical significance of *NPM1* mutation was further suggested. One thousand four hundred and eighty-five patients with AML were examined for *NPM1* exon 12 mutations using fragment analysis.[69] A 4-bp insert was detected in 408/1485 patients (27.5%). Sequence analysis revealed known mutations (type A, B and D) as well as 13 novel alterations in 229 of the cases analyzed. *NPM1* mutations were more prevalent in patients with normal karyotype (324/709; 45.7%) than in those with karyotype abnormalities (58/686, 8.5%; $P < 0.0001$), and were significantly associated with several clinical parameters (high bone marrow blasts, high white blood cell and platelet counts, women). *NPM1* alterations were associated with *FLT3/ITD* mutations, even if the cases analyzed were restricted to patients with normal karyotype. Analysis of the clinical impact in four groups (*NPM1* and *FLT3/ITD* single mutants, double mutants, and wild-type for both) revealed that patients having only an *NPM1* mutation had significantly better overall and disease-free survival and a lower cumulative incidence of relapse. In conclusion, *NPM1*-mutations represent a common genetic abnormality in adult AML. If not associated with *FLT3/ITD* mutations, mutant *NPM1* appears to identify patients with favorable response to treatment.

In summary, the *NPM1* mutation[61,65–70] is observed in a high percentage of *de novo* AML, and is associated with normal karyotype, *FLT3/ITD* and better response to chemotherapy (Table 2). It remains controversial whether the presence of *NPM1* mutation indicates a good prognosis, but it is clear that it indicates a good prognosis in patients without *FLT3/ITD*. Structurally, a newly generated NES sequence at the C-terminus is a common feature, although more than 20 different variant *NPM1* mutations have been identified.[63] How the acquired NES changes the function of NPM in addition to altering the subcellular localization should be studied. The second question is why only *FLT3* mutations frequently accompany the *NPM1* mutation. According to a Japanese study, D835 of *FLT3* is also frequently mutated in *NPM1*-mutated AML. One possibility is that mutated NPM may sequester some transcription factors associated with differentiation. Activated *FLT3* might tyrosine-phosphorylate cytoplasmic NPM, which has been observed in NPM–ALK. Another possibility is that mutated NPM lowers the replication or repair fidelity of DNA. Umekawa *et al.* reported that the C-terminal sequence of NPM is important for its elevated DNA polymerase alpha activity compared with the short isoform NPM1.2.[71] As described below, *NPM1* haploinsufficiency increases the number of centrosomes to more than two and causes karyotype abnormalities in mice.[30] However, *NPM1* mutations are observed exclusively in AML with normal karyotype, and *FLT3* is the sole target for mutation. Recently Colombo *et al.* showed that mutant NPM forms a direct complex with Arf but is unable to protect it from degradation.[29] AML cells and cell lines harboring mutant NPM have low levels of cytoplasmic Arf. Colombo *et al.* suggested that inactivation of Arf, a key regulator of the

doi: 10.1111/j.1349-7006.2006.00270.x

Table 2. Clinical relevance of *NPM1* mutation in acute myeloid leukemia

Reference	Total patients (%) (normal karyotype)	Nucleophosmin mt (%) (normal ka ryotype)	Prognosis			
			CR	OS	EFS	RFS
Falini *et al.*[61]	591	35.2	F	NA	NA	NA
	(230)	(61.7)				
Suzuki *et al.*[65]	257	24.9	F	NS	NA	U
	(97)	(47.4)				
Boissel *et al.*[70]	(106)	(47)	NS	NS	NS	NS
Dohner *et al.*[68]	(300)	(48)	NS	NS	NA	F
Schnittger *et al.*[66]	(401)	(52.9)	F	NS	F	NS
Verhaak *et al.*[67]	275	35	NA	NS	NS	NA
	(116)	(64)				
Thiede *et al.*[69]	1485	27.5	F	F	F	NA
	(709)	(45.7)			(DFS)	

CR, complete remission; DFS, disease-free survival; EFS, event-free survival; F, favorable; NS, not significant; OS, overall survival; RFS, relapse-free survival; U, unfavorable; NA, not analyzed.

p53-dependent cellular response to oncogene expression, might contribute to leukemogenesis in AML with mutated NPM. Further study is needed to clarify the underlying molecular mechanisms.

Haploinsufficiency and gene deletion in hematological malignancies

To study the function of NPM *in vivo*, Grisendi *et al.* generated *NPM1* heterozygous-null, hypomorphic-mutant and homozygous-null mice.[30] They observed that *NPM1* homozygous-null and hypomorphic mutants had aberrant organogenesis and died between embryonic days 11.5 and 16.5 owing to severe anemia resulting from defects in primitive hematopoiesis. They showed that *NPM1* inactivation leads to unrestricted centrosome duplication and genomic instability. Notably, *NPM1* heterozygous mice developed a hematological syndrome with features of human MDS. They concluded that their data uncovered an essential developmental role for NPM and implicated its functional loss in tumorigenesis and MDS pathogenesis.

According to the KO mice study, mutation or downregulation of *NPM1* as a tumor-suppressor gene may also be associated with human MDS. The evidence that *NPM1* is located on 5q35, which is deleted or rearranged in AML/MDS, suggests the loss of the *NPM1* gene in myeloid malignancies. Using fluorescence *in situ* hybridization and reverse transcription–polymerase chain reaction methods, Berger *et al.* analyzed eight AML/MDS cases with chromosomal breakpoints at 5q31–5q34.[72] Two bacterial artificial chromosome signals spanning the *NPM1* and *MLF1* genes were colocalized in three of the eight cases. However, the breakpoints were outside the *NPM1* gene in the remaining five cases, and one copy of the *NPM1* gene was deleted in three of the five. Further study is needed to determine the frequency and significance of *NPM1* deletion in the unbalanced translocation and chromosomal deletion.

Notably, the *NPM1* gene has a CpG island in its promoter region, which is potentially hypermethylated. However, no study has been reported about the methylation of the *NPM1* gene. The significance of promoter hypermethylation should also be investigated.

Conclusions and future directions

The *NPM1* gene is one of the most frequent targets for deletion and insertion mutations in addition to acting as a component of fusion genes. In fusion genes, translocation of the *NPM1* gene on the 5′ side is associated with ectopic expression, aberrant subcellular localization and oligomerization of the partner gene products. However, the biological significance of the *NPM1* gene mutation at exon 12 remains unclear. It may be associated with a mutator phenotype, dysregulated transcription or apoptosis. One interesting issue is altered nuclear–cytoplasmic trafficking of mutant NPM. The export system of mutant NPM might be a candidate for targeted therapy for NPM-mutated AML. Clarification of the expression and subcellular localization of NPM-interacting proteins such as p53, MDM2 and Arf in NPM-mutated AML would help to further our understanding of the pathogenesis of this disease. It would also yield insights into the masked function of NPM in myeloid hematopoiesis. The interaction between *FLT3* and *NPM1* mutations is another important issue for future studies. The evidence that *FLT3* and *NPM1* mutations are observed in a variety of types of AML from M0 to M7 (except M3) raises the question of what determines the phenotype of AML from M0 to M7. Thus, one discovery generates 10 more questions.

References

1 Lischwe M, Smetana K, Olson M *et al.* Protein-C23 and protein-B23 are the major nucleolar silver staining proteins. *Life Sci* 1979; **25**: 701–8.
2 Feuerstein N, Spiegel S, Mond JJ. The nuclear matrix protein, numatrin (B23), is associated with growth factor-induced mitogenesis in Swiss 3T3 fibroblasts and with T lymphocyte proliferation stimulated by lectins and anti-T cell antigen receptor antibody. *J Cell Biol* 1988; **107**: 1629–42.
3 Chan W-Y, Liu Q-R, Borjigin J *et al.* Characterization of the cDNA encoding human nucleophosmin and studies of its role in normal and abnormal growth. *Biochemistry* 1989; **28**: 1033–9.
4 Dalenc F, Drouet J, Ader I *et al.* Increased expression of a COOH-truncated nucleophosmin resulting from alternative splicing is associated with cellular resistance to ionizing radiation in HeLa cells. *Int J Cancer* 2002; **100**: 662–8.
5 International Human Genome Sequencing Consortium. Finishing the euchromatic sequence of the human genome. *Nature* 2004; **431**: 931–45.
6 Wang D, Umekawa H, Olson MO. Expression and subcellular locations of two forms of nucleolar protein B23 in rat tissues and cells. *Cell Mol Biol Res* 1993; **39**: 33–42.
7 Wang W, Budhu A, Forgues M, Wang XW. Temporal and spatial control of nucleophosmin by the Ran–Crm1 complex in centrosome duplication. *Nat Cell Biol* 2005; **7**: 823–30.
8 Morris SW, Xue L, Ma Z, Kinney MC. Alk+ CD30+ lymphomas: a distinct molecular genetic subtype of non-Hodgkin's lymphoma. *Br J Haematol* 2001; **113**: 275–95.
9 Pandolfi PP. *PML*, *PLZF* and *NPM* genes in the molecular pathogenesis of acute promyelocytic leukemia. *Haematologica* 1996; **81**: 472–82.
10 Yoneda-Kato N, Look AT, Kirstein MN *et al.* The t(3;5) (q25.1;q34) of myelodysplastic syndrome and acute myeloid leukemia produces a novel fusion gene, *NPM–MLF1*. *Oncogene* 1996; **12**: 265–75.
11 Okuda M. The role of nucleophosmin in centrosome duplication. *Oncogene* 2002; **21**: 6170–4.

12 Colombo E, Marine JC, Danovi D, Falini B, Pelicci PG. Nucleophosmin regulates the stability and transcriptional activity of p53. *Nat Cell Biol* 2002; **4**: 529–33.
13 Szebeni A, Herrera JE, Olson MO. Interaction of nucleolar protein B23 with peptides related to nuclear localization signals. *Biochemistry* 1995; **34**: 8037–42.
14 Borer RA, Lehner CF, Eppenberger HM, Nigg EA. Major nucleolar proteins shuttle between nucleus and cytoplasm. *Cell* 1989; **56**: 379–90.
15 Dutta S, Akey IV, Dingwall C *et al.* The crystal structure of nucleoplasmin-core: implications for histone binding and nucleosome assembly. *Mol Cell* 2001; **8**: 841–53.
16 Huang N, Negi S, Szebeni A, Olson MO. Protein NPM3 interacts with the multifunctional nucleolar protein B23/nucleophosmin and inhibits ribosome biogenesis. *J Biol Chem* 2005; **280**: 5496–502.
17 Kondo T, Minamino N, Nagamura-Inoue T, Matsumoto M, Taniguchi T, Tanaka N. Identification and characterization of nucleophosmin/B23/numatrin which binds the anti-oncogenic transcription factor IRF-1 and manifests oncogenic activity. *Oncogene* 1997; **15**: 1275–81.
18 Hsu CY, Yung BY. Over-expression of nucleophosmin/B23 decreases the susceptibility of human leukemia HL-60 cells to retinoic acid-induced differentiation and apoptosis. *Int J Cancer* 2000; **88**: 392–400.
19 Kurki S, Peltonen K, Latonen L *et al.* Nucleolar protein NPM interacts with HDM2 and protects tumor suppressor protein p53 from HDM2-mediated degradation. *Cancer Cell* 2004; **5**: 465–75.
20 Sirri V, Roussel P, Gendron MC, Hernandez-Verdun D. Amount of the two major Ag-NOR proteins, nucleolin and protein B23, is cell-cycle dependent. *Cytometry* 1997; **28**: 147–56.
21 Okuda M, Horn HF, Tarapore P *et al.* Nucleophosmin/B23 is a target of CDK2/cyclin E in centrosome duplication. *Cell* 2000; **103**: 127–40.
22 Okuda M. The role of nucleophosmin in centrosome duplication. *Oncogene* 2002; **21**: 6170–4.
23 Cha H, Hancock C, Dangi S, Maiguel D, Carrier F, Shapiro P. Phosphorylation regulates nucleophosmin targeting to the centrosome during mitosis as detected by cross-reactive phosphorylation-specific MKK1/MKK2 antibodies. *Biochem J* 2004; **378**: 857–65.
24 Wu MH, Yung BY. UV stimulation of nucleophosmin/B23 expression is an immediate-early gene response induced by damaged DNA. *J Biol Chem* 2002; **277**: 48 234–40.
25 Zhang Y, Xiong Y. Control of p53 ubiquitination and nuclear export by MDM2 and ARF. *Cell Growth Diff* 2001; **12**: 175–86.
26 Brady SN, Yu Y, Maggi LB Jr, Weber JD. ARF impedes NPM/B23 shuttling in an Mdm2-sensitive tumor suppressor pathway. *Mol Cell Biol* 2004; **24**: 9327–38.
27 Bertwistle D, Sugimoto M, Sherr CJ. Physical and functional interactions of the Arf tumor suppressor protein with nucleophosmin/B23. *Mol Cell Biol* 2004; **24**: 985–96.
28 Korgaonkar C, Hagen J, Tompkins V *et al.* Nucleophosmin (B23) targets ARF to nucleoli and inhibits its function. *Mol Cell Biol* 2005; **25**: 1258–71.
29 Colombo E, Bonetti P, Lazzerini Denchi E *et al.* Nucleophosmin is required for DNA integrity and p19Arf protein stability. *Mol Cell Biol* 2005; **25**: 8874–86.
30 Grisendi S, Bernardi R, Rossi M *et al.* Role of nucleophosmin in embryonic development and tumorigenesis. *Nature* 2005; **437**: 147–53.
31 Sugimoto M, Kuo ML, Roussel MF, Sherr CJ. Nucleolar Arf tumor suppressor inhibits ribosomal RNA processing. *Mol Cell* 2003; **11**: 415–24.
32 Itahana K, Bhat KP, Jin A *et al.* Tumor suppressor ARF degrades B23, a nucleolar protein involved in ribosome biogenesis and cell proliferation. *Mol Cell* 2003; **12**: 1151–64.
33 Jaffe ES, Harris NL, Stein H, Vardiman JW, eds. *Pathology and Genetics of Tumors of Haematopoietic and Lymphoid Tissues.* Lyon, France: IARC Press, 2001.
34 Duyster J, Bai RY, Morris SW. Translocations involving anaplastic lymphoma kinase (ALK). *Oncogene* 2001; **20**: 5623–37.
35 Morris SW, Kirstein MN, Valentine MB *et al.* Fusion of a kinase gene, *ALK*, to a nucleolar protein gene, *NPM*, in non-Hodgkin's lymphoma. *Science* 1994; **263**: 1281–4.
36 Pulford K, Lamant L, Espinos E *et al.* The emerging normal and disease-related roles of anaplastic lymphoma kinase. *Cell Mol Life Sci* 2004; **61**: 2939–53.
37 Slupianek A, Nieborowska-Skorska M, Hoser G *et al.* Role of phosphatidylinositol 3-kinase-Akt pathway in nucleophosmin/anaplastic lymphoma kinase-mediated lymphomagenesis. *Cancer Res* 2001; **61**: 2194–9.
38 Ruchatz H, Coluccia AM, Stano P, Marchesi E, Gambacorti-Passerini C. Constitutive activation of Jak2 contributes to proliferation and resistance to apoptosis in NPM/ALK-transformed cells. *Exp Hematol* 2003; **31**: 309–15.
39 Turner SD, Alexander DR. What have we learnt from mouse models of NPM–ALK-induced lymphomagenesis? *Leukemia* 2005; **19**: 1128–34.
40 Stein H, Foss HD, Durkop H *et al.* CD30(+) anaplastic large cell lymphoma: a review of its histopathologic, genetic, and clinical features. *Blood* 2000; **96**: 3681–95.
41 Horie R, Watanabe T, Morishita Y *et al.* Ligand-independent signaling by overexpressed CD30 drives NF-κB activation in Hodgkin–Reed–Sternberg cells. *Oncogene* 2002; **21**: 2493–503.
42 Horie R, Watanabe M, Ishida T *et al.* The *NPM–ALK* oncoprotein abrogates CD30 signaling and constitutive NF-κB activation in anaplastic large cell lymphoma. *Cancer Cell* 2004; **5**: 353–64.
43 Cordell JL, Pulford KA, Bigerna B *et al.* Detection of normal and chimeric nucleophosmin in human cells. *Blood* 1999; **93**: 632–42.
44 Drexler HG, Gignac SM, von Wasielewski R, Werner M, Dirks WG. Pathobiology of *NPM–ALK* and variant fusion genes in anaplastic large cell lymphoma and other lymphomas. *Leukemia* 2000; **14**: 1533–59.
45 Piazza F, Gurrieri C, Pandolfi PP. The theory of APL. *Oncogene* 2001; **20**: 7216–22.
46 Zelent A, Guidez F, Melnick A, Waxman S, Licht JD. Translocations of the *RARα* gene in acute promyelocytic leukemia. *Oncogene* 2001; **20**: 7186–203.
47 Grimwade D, Biondi A, Mozziconacci MJ *et al.* Characterization of acute promyelocytic leukemia cases lacking the classic t(15;17): results of the European Working Party. *Blood* 2000; **96**: 1297–308.
48 Corey SJ, Locker J, Oliveri DR *et al.* A non-classical translocation involving 17q12 (retinoic acid receptor α) in acute promyelocytic leukemia (APML) with atypical features. *Leukemia* 1994; **8**: 1350–3.
49 Redner RL, Rush EA, Faas S, Rudert WA, Corey SJ. The t(5;17) variant of acute promyelocytic leukemia expresses a nucleophosmin–retinoic acid receptor fusion. *Blood* 1996; **87**: 882–6.
50 Redner RL, Corey SJ, Rush EA. Differentiation of t(5;17) variant acute promyelocytic leukemic blasts by all-trans retinoic acid. *Leukemia* 1997; **11**: 1014–16.
51 Redner RL, Chen JD, Rush EA, Li H, Pollock SL. The t(5;17) acute promyelocytic leukemia fusion protein NPM–RAR interacts with co-repressor and co-activator proteins and exhibits both positive and negative transcriptional properties. *Blood* 2000; **95**: 2683–90.
52 Sternsdorf T, Phan VT, Maunakea ML *et al.* Forced retinoic acid receptor α homodimers prime mice for APL-like leukemia. *Cancer Cell* 2006; **9**: 81–94.
53 Cheng GX, Zhu XH, Men XQ *et al.* Distinct leukemia phenotypes in transgenic mice and different corepressor interactions generated by promyelocytic leukemia variant fusion genes *PLZF–RARα* and *NPM–RARα*. *Proc Natl Acad Sci USA* 1999; **96**: 6318–23.
54 Dyck JA, Maul GG, Miller WH Jr, Chen JD, Kakizuka A, Evans RM. A novel macromolecular structure is a target of the promyelocyte–retinoic acid receptor oncoprotein. *Cell* 1994; **76**: 333–43.
55 Raelson JV, Nervi C, Rosenauer A *et al.* The PML/RARα oncoprotein is a direct molecular target of retinoic acid in acute promyelocytic leukemia cells. *Blood* 1996; **88**: 2826–32.
56 Yoshida H, Kitamura K, Tanaka K *et al.* Accelerated degradation of PML–retinoic acid receptor alpha (PML–RARA) oncoprotein by all-trans-retinoic acid in acute promyelocytic leukemia: possible role of the proteasome pathway. *Cancer Res* 1996; **56**: 2945–8.
57 Rush EA, Schlesinger KW, Watkins SC, Redner RL. The NPM–RAR fusion protein associated with the t(5;17) variant of APL does not interact with PML. *Leuk Res* 2006; **30**: 979–86.
58 Winteringham LN, Kobelke S, Williams JH, Ingley E, Klinken SP. Myeloid leukemia factor 1 inhibits erythropoietin-induced differentiation, cell cycle exit and p27Kip1 accumulation. *Oncogene* 2004; **23**: 5105–9.
59 Hanissian SH, Akbar U, Teng B *et al.* cDNA cloning and characterization of a novel gene encoding the MLF1-interacting protein MLF1IP. *Oncogene* 2004; **23**: 3700–7.
60 Falini B, Bigerna B, Pucciarini A *et al.* Aberrant subcellular expression of nucleophosmin and NPM–MLF1 fusion protein in acute myeloid leukaemia carrying t(3;5): a comparison with NPMc+ AML. *Leukemia* 2006; **20**: 368–71.
61 Falini B, Mecucci C, Tiacci E *et al.* Gimema Acute Leukemia Working Party. Cytoplasmic nucleophosmin in acute myelogenous leukemia with a normal karyotype. *N Engl J Med* 2005; **352**: 254–66.
62 Nakagawa M, Kameoka Y, Suzuki R. Nucleophosmin in acute myelogenous leukemia. *N Engl J Med* 2005; **352**: 1819–20.
63 Falini B, Bolli N, Shan J *et al.* Both carboxy-terminus NES motif and mutated tryptophan(s) are crucial for aberrant nuclear export of nucleophosmin leukemic mutants in NPMc+ AML. *Blood* 2006; **107**: 4514–23.
64 Grisendi S, Pandolfi PP. NPM mutations in acute myelogenous leukemia. *N Engl J Med* 2005; **352**: 291–2.
65 Suzuki T, Kiyoi H, Ozeki K *et al.* Clinical characteristics and prognostic implications of NPM1 mutations in acute myeloid leukemia. *Blood* 2005; **106**: 2854–61.
66 Schnittger S, Schoch C, Kern W *et al.* Nucleophosmin gene mutations are predictors of favorable prognosis in acute myelogenous leukemia with a normal karyotype. *Blood* 2005; **106**: 3733–9.
67 Roel GWV, Chantal SG, Wim van P *et al.* Mutations in nucleophosmin (NPM1) in acute myeloid leukemia (AML): association with other gene

doi: 10.1111/j.1349-7006.2006.00270.x

abnormalities and previously established gene expression signatures and their favorable prognostic significance. *Blood* 2005; **106**: 3747–54.
68 Konstanze D, Richard FS, Marianne H *et al.* Mutant nucleophosmin (NPM1) predicts favorable prognosis in younger adults with acute myeloid leukemia and normal cytogenetics: interaction with other gene mutations. *Blood* 2005; **106**: 3740–6.
69 Christian T, Sina K, Eva C *et al.* Prevalence and prognostic impact of NPM1 mutations in 1485 adult patients with acute myeloid leukemia (AML) *Blood* 2006; **107**: 4011–20.
70 Boissel N, Renneville A, Biggio V *et al.* Prevalence, clinical profile, and prognosis of NPM mutations in AML with normal karyotype. *Blood* 2005; **106**: 3618–20.
71 Umekawa H, Sato K, Takemura M *et al.* The carboxyl terminal sequence of nucleolar protein B23.1 is important in its DNA polymerase α-stimulatory activity. *J Biochem (Tokyo)* 2001; **130**: 199–205.
72 Berger R, Busson M, Baranger L *et al.* Loss of the *NPM1* gene in myeloid disorders with chromosome 5 rearrangements. *Leukemia* 2006; **20**: 319–21.
73 Namboodiri VM, Akey IV, Schmidt-Zachmann MS, Head JF, Akey CW. The structure and function of *Xenopus* NO38-core, a histone chaperone in the nucleolus. *Structure* 2004; **12**: 2149–60.

ELSEVIER

Cancer Genetics and Cytogenetics 169 (2006) 1–11

CANCER GENETICS AND CYTOGENETICS

Establishment of a myeloid leukemia cell line, TRL-01, with *MLL-ENL* fusion gene

Manabu Ninomiya[a,1], Akihiro Abe[a,1], Toshiya Yokozawa[b], Kazutaka Ozeki[a], Kazuhito Yamamoto[c], Mamoru Ito[d], Masafumi Ito[e], Hitoshi Kiyoi[f], Nobuhiko Emi[a], Tomoki Naoe[a,*]

[a]*Department of Hematology, Nagoya University Graduate School of Medicine, 65 Tsurumai-cho, Showa-ku, Nagoya 466-8550, Japan*
[b]*Division of Hematology, Nagoya Medical Center, National Hospital Organization, 4-1-1 Sannomaru, Naka-Ku, Nagoya, Japan*
[c]*Department of Preventive Medicine/Biostatics and Medical Decision Making, Nagoya University Graduate School of Medicine, Nagoya, Japan*
[d]*Central Institute for Experimental Animals, 1430 Nogawa, Miyamae-ku, Kawasaki, Japan*
[e]*Department of Pathology, Japanese Red Cross Nagoya First Hospital, 3-35 Michisita-cho, Nakamura-ku, Nagoya, Japan*
[f]*Department of Infectious Diseases, Nagoya University Hospital, 65 Tsuramai-cho, Showa-ku, Nagoya, Japan*

Received 21 July 2005; received in revised form 8 September 2005; accepted 9 September 2005

Abstract We established a leukemia cell line derived from therapy-related acute myeloid leukemia with the t(11;19) by xenotransplantation into the NOD/SCID mouse with IL-2Rγ_c−/− (NOG mouse). The cell line, TRL-01, could be serially transplanted from mouse to mouse and also grown in an adherence-dependent manner on a murine bone marrow stroma cell line, HESS-5. TRL-01 had the same immunophenotype as the original leukemia cells: positive for CD13, CD33, CD11a, CD18, CD29, CD49d, CD49e, CD54, CD62L, and CD117, and negative for CD3, CD4, CD8, CD19, CD34, CD41a, CD41b, CD135, and myeloperoxidase. Translocation (11;19)(q23;p13) in both the original sample and TRL-01 generated *MLL-ENL* chimeric transcripts joining exon 6 and exon 4, respectively, which has a novel isoform. In cultures of TRL-01, addition of GM-CSF, SCF, and G-CSF and adhesion to fibronectin-coated plates promoted transient proliferation and survival, although they did not support long-term culture. Subcutaneous injection caused a tumor to form only when HESS-5 was coinjected at the same site. These results suggest that TRL-01 is a useful cell line for studying not only the leukemia-related biology of *MLL-ENL* but also the intercellular association between leukemia and stroma.

1. Introduction

Leukemia cell lines are indispensable tools in the study of research of leukemia. Many cell lines have contributed to advances in basic biology or to therapeutic development [1]. Nevertheless, the cell lines are different from leukemia cells in vivo. For example, leukemia cells removed from their environment (e.g., bone marrow [BM]) usually undergo apoptosis within a few weeks even if cultured carefully. Moreover, during the process of establishing cell lines, a variety of events may intrude, singly or in combination: a small population of leukemia cells may be selected, transcriptional control may change, or genomic alterations may be accumulated [2,3]. A new culture system is needed, one that is more similar to the native environment.

Recently, immunodeficient mice have been generated to study leukemia in terms of cellular origin, pathogenesis, and approaches to therapy. Such models have the advantage of allowing the cellular biology of leukemia to be investigated, especially the leukemia–microenvironment interaction [4–6]. So far, however, it has been impossible to maintain human leukemia cells long term by passage from mouse to mouse, although there are many reports on xenotransplantation of human leukemia into mice. To generate more immunodeficient mice, the common γ chain gene or β_2-microglobulin gene has been knocked out in NOD/SCID mice [7]. In cord blood xenotransplantation, engraftment with excellent efficacy and differentiation into all lineages, including T cells, were observed [8]; however, the efficacy of engraftment using clinical samples has not fully been

[1] These authors are equal contributors.

* Corresponding author. Tel. and fax: +81-52-744-2136.
E-mail address: naoe@med.nagoya-u.ac.jp (T. Naoe).

0165-4608/06/$ – see front matter © 2006 Elsevier Inc. All rights reserved.
doi:10.1016/j.cancergencyto.2005.09.008

investigated. We have transplanted fresh leukemia cells into NOG mice to establish an animal model of leukemia.

Here we established a leukemia cell line derived from therapy-related acute myeloid leukemia with the t(11;19) by xenotransplantation into NOG mice. The cell line could be serially transplanted from mouse to mouse and also grown in an adherence-dependent manner on a murine bone marrow stroma cell line, HESS-5.

2. Materials and methods

2.1. Patient

A 34-year-old Japanese woman was admitted to our hospital because of pancytopenia and detection of peripheral blasts in March 2003. From March 1997 through April 2001, she was treated with a succession of chemotherapies including etoposide (a total dose of 32.9 g), actinomycin-D, methotrexate, cisplatin, carboplatin, cyclophosphamide, ifosfamide, and vincristine against recurrent choriocarcinoma. Her BM blasts were peroxidase-negative and CD13+, CD33+, CD3−, CD4−, CD5−, CD56−, CD7+, CD19−, CD34−, CD14−, CD11b−, CD10−, CD41b−, CD41a−. The karyotype was 46,XX,t(11;19)(q23;p13),add(12)(p11)[10]/46, idem,i(21)(q10)[5]/46,idem,add(21)(q22)[5] in 20 metaphases examined. She was diagnosed with topoisomerase II inhibitor-related acute myeloid leukemia (AML) according to the WHO classification. Hematological remission was achieved by chemotherapy with idarubicin and cytarabine, but the truncal skin was involved 2 months later. She received an allogeneic peripheral stem cell transplantation in July 2003, but died of graft failure and pneumonia in September 2003.

2.2. Cells

The BM cells from the patient were collected after obtaining informed consent. Mononuclear cells (MNC) were separated by Ficoll-Paque Plus (Amersham Bioscience, Uppsala, Sweden) density-gradient centrifugation, and used as BM MNCs for the transplantation procedure. Some of the cells were cultivated in RPMI 1640 medium (Gibco-BRL, Gaithersburg, MD) supplied with 20 % fetal bovine serum (Gibco-BRL), 100 IU/mL of penicillin G (Meiji Seika, Tokyo, Japan), and 100 μg/mL of streptomycin (Meiji Seika). The murine BM stroma cell line MS-5 was maintained in α-minimum essential medium (α-MEM; Gibco-BRL) supplemented with 20% horse serum (Gibco-BRL), 100 IU/mL of penicillin G, and 100 μg/mL of streptomycin. The murine BM stroma cell line HESS-5 was maintained in Dulbecco's minimal essential medium (DMEM; Gibco-BRL) supplemented with 10% horse serum, 100 IU/mL of penicillin G, and 100 μg/mL of streptomycin. The monkey kidney-derived epithelial-like cell line COS-7, human kidney-derived epithelial-like cell line 293T, and murine embryo-derived fibroblast-like cell line NIH3T3 were maintained in DMEM supplemented with 10% fetal bovine serum, 100 IU/mL of penicillin G, and 100 μg/mL of streptomycin. The newborn murine calvaria-derived fibroblast-like cell line OP9 was maintained in α-MEM supplemented with 20% fetal bovine serum, 100 IU/mL of penicillin G, and 100 μg/mL of streptomycin. Human precursor B-cell ALL cell line RS4;11 with t(4;11) was obtained from the American Type Culture Collection (ATCC, Rockville, MD). The cell lines were cultivated in RPMI-1640 medium supplemented with 10% fetal bovine serum, 100 IU/mL of penicillin G, and 100 μg/mL of streptomycin.

2.3. Mice and transplantation procedure

NOG mice, generated by backcrossing NOD/SCID mice with C57BL6J-γ_c−/− mice as described [7], were maintained at the Central Institute for Experimental Animals (Kawasaki, Japan). The BM MNCs (2×10^6 cells) were injected into nonirradiated 7- to 8-week-old male mice via a tail vein. In the serial passage experiment, the spleen was extirpated from the engrafted mice after ether anesthesia. Cell suspension was prepared from the spleen, then it was adjusted to 2×10^6 cells and injected into nonirradiated 7- to 8-week-old male mice via a tail vein. We repeated the procedure at 8-week intervals. The animal experiments were approved by the institutional ethics committee for Laboratory Animal Research, Nagoya University School of Medicine and were performed according to the guidelines of the Institute.

2.4. Phenotypic analyses

Flow-cytometric analyses were performed according to a method described below. NOG mice at 8 weeks after transplantation were killed under ether anesthesia, and then the major organs were removed. Cell suspensions from BM and spleen were prepared and subjected to flow cytometry. To detect human cells from the tissues, a multicolor cytometric analysis was performed using FACScalibur (Becton Dickinson [BD], Franklin Lakes, NJ), according to the manufacturer's direction. Samples were mixed and incubated with an appropriate volume of antibodies for 30 minutes on ice. These cells were examined by staining with a combination of 7-AAD (BD PharMingen) for the live gate, and either or both of phycoerythrin (PE)-conjugated antibody and fluorescein isothiocyanate (FITC)-conjugated antibody. The PE-conjugated antibodies used were anti-human CD3, CD19, CD33, CD34 antibodies (BD, San Jose, CA), anti-human CD56 antibody (BD Pharmingen). The FITC-conjugated antibody was anti-human CD45 antibody (BD). FITC and PE-labeled isotype control antibodies (BD) were also used.

For the evaluation of the surface marker of TRL-01, the cells were stained with a combination of PerCP-conjugated anti-human CD45 antibody (BD) for the CD45 gate and either or both of PE-conjugated antibodies and FITC-conjugated antibody. The PE-conjugated antibodies used were anti-human CD11b, CD13, CD14, CD18, CD29,

CD44, CD49d, CD49e antibodies (BD), and anti-human CD117, CD135 antibodies (Beckman Coulter, San Jose, CA). The FITC-conjugated antibody used was anti-human CD41 antibody (BD). An additional reaction with FITC and PE-labeled isotype control antibodies (BD) was performed as a negative control. Analyses were performed using Cell Quest software (BD).

2.5. Karyotype and dual-color fluorescence in situ hybridization analyses

Karyotyping was performed as described previously [9]. Briefly, the BM or spleen cells from NOG mice were cultured for 24 hours. Twenty G-banded metaphases were analyzed according to standard procedures. Dual-color fluorescence in situ hybridization (DC-FISH) analyses were performed as described previously [9], using an LSI MLL dual-color break-apart rearrangement probe consisting of a 350-kbp portion of the *MLL* gene breakpoint cluster region (bcr) labeled in SpectrumGreen and an ~190-kbp portion largely telomeric of the bcr labeled in SpectrumOrange (Vysis, Abbott Laboratories, Abbott Park, IL). The translocation signals were evaluated using a fluorescence microscope with triple-pass filters (Nikon, Tokyo, Japan). At least 500 cells without damaged nuclei were blindly counted in each sample. Less than 1% of the total cell population failed to show hybridization. Only those spots with a similar size, intensity, and shape were counted. A fusion spot was scored as a normal *MLL* allele (negative for the MLL translocation); split signals of green and orange were scored as positive for the *MLL* translocation.

2.6. Reverse transcription-polymerase chain reaction (RT-PCR)

For reverse transcription polymerase chain reaction (RT-PCR), total RNA was prepared from the spleen of mouse and BM MNCs using a QIAamp RNA blood mini kit (Qiagen, Chatsworth, CA) as previously described [10]. Briefly, cDNA was synthesized from extracted RNA using random primer, dNTP, Superscript II (reverse transcriptase; Gibco-BRL), dithiothreitol, and $MgCl_2$ in a final volume of 20 μL at 42°C for 40 min. The 1 μL cDNA was amplified with 0.2 mmol/L dNTP, 1.25 U AmpliTaq Gold (DNA polymerase; Perkin-Elmer, Norwalk, CT), and 0.5 μmol/L primers in 50-μL reaction volumes using a GeneAmp PCR System 9600 (Perkin Elmer). Each thermal cycle to detect *MLL-ENL* [11], *MLL-ELL* [12], or *MLL-MEN* [13] was performed according to the described method with 35 cycles. Primers were synthesized by Nihon Gene Research Lab (Sendai, Japan); for the sequences of the primers in *MLL-ENL*, see the Supplemental Data section. PCR products were separated on 1.5% agarose gels and visualized by ethidium bromide staining and photographed on a UV transilluminator FASIII (Toyobo, Tokyo, Japan).

2.7. cDNA panhandle PCR

Panhandle PCR was performed with the described method [14,15]. Total RNA was prepared from TRL-01 using a QIAamp RNA blood mini kit (Qiagen). First-strand cDNAs were synthesized from 1 μg of total RNA by using the Superscript preamplification system (Life Technologies, Grand Island, NY), using *MLL*-random hexamer oligonucleotides (5′-CCTGAATCCAAA-CAGGCCACCACTCCAGCTTC-NNNNNN-3′); the *MLL* sequence in the oligonucleotides corresponded to breakpoint cluster region (bcr) cDNA positions 92–123 in exon 5. Two microliters of first-strand cDNAs was added to a 45.5-μL mixture containing 1.75 units of AmpliTaq Gold (DNA polymerase; Perkin Elmer), 385 μmol/L of each dNTP, 1.1× buffer, and 12.5 pmol of *MLL* primer 1. The mixture was heated to 80°C for 5 min before the cDNAs were added.

Primer 1 corresponded to *MLL* bcr cDNA positions 34–55 in exon 5 (5′-TCCTCCACGAAAGCCCGTC-GAG-3′), upstream of the *MLL* sequence in the oligonucleotides used to synthesize the first-strand cDNAs. To achieve primer 1 extension, the mixture was denatured at 94°C for 1 min. This was followed by 1 cycle at 94°C for 10 sec and 68°C for 7 min. The sample was heated again to 80°C for 5 min and 2.5 μL (12.5 pmol) of *MLL* primer 2 was added.

Primer 2 corresponded to *MLL* bcr cDNA positions 136–158 in exon 5 (5′-TCAAGCAGGTCTCCCAGCCAG-CAC-3′), downstream of the *MLL* sequence in the oligonucleotides used to synthesize the first-strand cDNAs. The final 50-μL PCR mixtures contained 350 μmol/L of each dNTP and 1× buffer.

PCR with primers 1 and 2, including the 7-min elongation and the incremental increase in the elongation period, was performed as described. One microliter of the products was used in nested PCR with primers 3 (5′-GGAAAA-GAGTGAAGAAGGGAATGTCTCGG-3′) and 4 (5′-GTGGTCATCCCGCCTCAGCCAC-3′) corresponding to *MLL* bcr cDNA positions 55–83 and 159–179 in exon 5. Conditions were the same as described above.

Panhandle PCR products were cloned into the plasmid vector, pBluescript SK(−) (Stratagene, La Jolla, CA), and the transformation was performed with DH5α cells (Life Technologies) according to the manufacturer's instructions. Subclones containing cDNA panhandle PCR products were identified by PCR with *MLL* primer 2 and primer 4. The resulting PCR fragments were sequenced by using the BigDye terminator cycle sequencing kit (Applied Biosystems, Foster City, CA) and analyzed with an ABI PRISM 310 genetic analyzer (Applied Biosystems).

For the detection of *MLL-ENL* transcripts of TRL-01, RT-PCR was performed. Total RNA was converted to single-stranded cDNA using oligo(dT) primers and MMLV-RT (Perkin Elmer). The resulting first-strand cDNA was amplified with *MLL* primer 4 and *ENL* primer 1 (5′-GGATGGTTTGGTCTTCTTGGGGTCAG-3′) by the use

of a Perkin Elmer GeneAmp 2400 thermocycler (Applied Biosystems).

2.8. Pathological examination

To evaluate morphological status, the extracted tissues were fixed with 10% formalin, and 4-μm sections mounted on slides were stained with hematoxylin and eosin (H&E). For immunohistochemical staining of human CD45, a LSAB2 system (DAKO Cytomation, Kyoto, Japan) using anti-human CD45 mouse monoclonal antibody (DAKO Cytomation) was used according to the instructions of an automatic immunohistochemical stainer (DAKO Cytomation).

2.9. Stroma-dependent growth in vivo

NOG mice were subcutaneously injected with 2×10^6 cells of TRL-01 and 6×10^4 cells of HESS-5 into dorsal regions. As controls, either 2×10^6 cells of TRL-01 alone or 6×10^4 cells of HESS-5 alone were similarly injected. The major axis (D, in mm) and minor axis (d, in mm) of the subcutaneous tumor was measured with vernier calipers, and the weight (mg) of the tumor was calculated with the formula $D \times d^2/2$ [16]. Human CD45 immunostaining and RT-PCR with *MLL-ENL* primers was performed to confirm the subcutaneous tumor to be involving of TRL-01 cells.

2.10. Proliferation and survival of the cells

The proliferation of the cells was profiled with a hemocytometer. The survival of the cells was examined using the trypan blue dye exclusion method. The requirement of direct adherence was estimated as follows. TRL-01 cells, adjusted to 1×10^5/mL, were seeded into a 6-well culture plate (BD), which was precultured with 5×10^3/mL of HESS-5 cells. The cell number and survival was estimated at 0, 3, and 7 days. After a BD cell culture insert (6-well format), which is a 0.4-μm porous membrane, had settled in the HESS-5 monolayer of the 6-well plate, 5×10^5 TRL-01 cells were seeded onto the insert. Total volume was adjusted to 5 mL in each well. The proliferation and survival was estimated during 7 days and was compared with the culture without a cell culture insert as a control. To investigate the

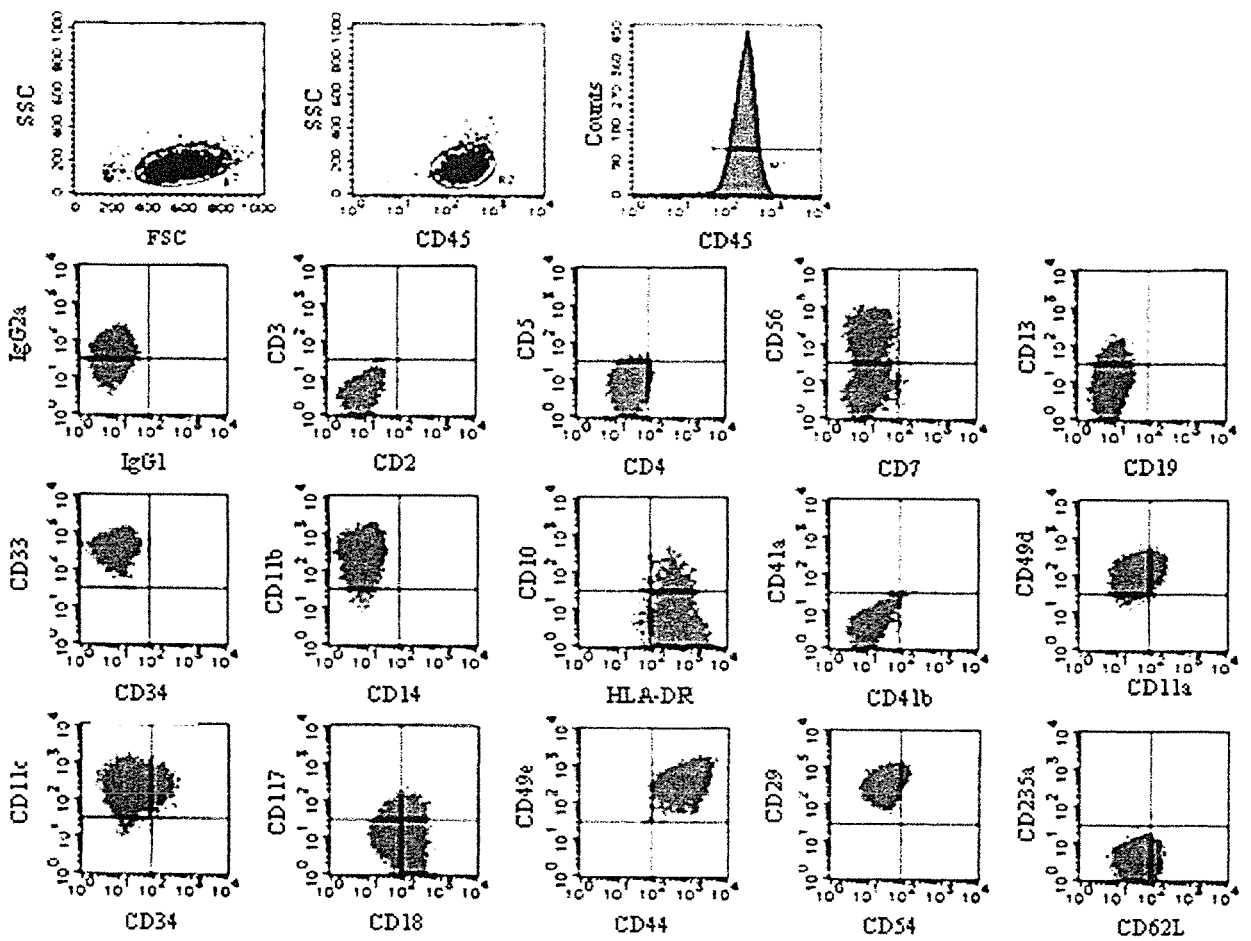

Fig. 1. Flow-cytometric analyses of the cells from the spleen of an engrafted NOG mouse 8 weeks after transplantation of BM MNCs from the AML M0 patient.

effect of the growth factors, TRL-01 cells were adjusted to 1×10^5/mL, and seeded into BioCoat (human fibronectin coated 6-well plate; BD). Then, 50 ng/mL of stem cell factor (SCF; Kirin, Tokyo, Japan), granulocyte macrophage-colony stimulating factor (GM-CSF; Kirin), granulocyte-colony stimulating factor (G-SCF; Kirin), thrombopoietin (TPO; Kirin), or erythropoietin (EPO; Kirin) was added to the culture. Differentiation was evaluated by flow-cytometric analysis using the labeled antibodies, and morphological changes of TRL-01 cells were detected by examining cytospin specimens subjected to May–Gruenwald's Giemsa staining and peroxidase–Giemsa staining.

2.11. Apoptosis detection

Apoptosis of TRL-01 cells was examined with FACScalibur using an Annexin V-FITC apoptosis detection kit (BD Pharmingen) according to the manufacturer's directions. Briefly, TRL-01 cells, adjusted to 1×10^5/mL, were seeded into a 6-well culture plate (BD), which was precultured with 5×10^3/mL of HESS-5 cells, BioCoat, or nontreated plate. The percentage of apoptosis was estimated using FACScalibur (BD) at 7 days. Analyses were performed using Cell Quest software (BD).

2.12. Statistics

Each experiment of proliferation, survival, and detection of apoptosis was repeated three times. Significant differences were calculated using the Student's *t*-test.

3. Results

The BM MNCs prepared from the leukemia patient were transplanted into NOG mice. Eight weeks later, the BM cells were replaced with human CD45-positive cells, which were passed at 8-week intervals for more than one year. The cells collected from the BM or spleen did not proliferate alone in medium but could be cultured on a BM stroma cell line, HESS-5. The doubling time was in the range of 3–4 days. TRL-01 in culture was able to be passed every week. This cell line was designated as TRL-01 and used for the subsequent experiments.

TRL-01 showed a basophilic cytoplasm, had round or indented nuclei with a fine nucleoreticulum, and was found to be negative for peroxidase and weakly positive for α-naphthyl acetate esterase. TRL-01 was found to be positive for myeloid markers of CD13 and CD33 and negative for lymphoid, monocytoid, erythroid, and megakaryocytoid markers, which was the same as the original leukemia cells ($CD13^+$, $CD33^+$, $CD3^-$, $CD4^-$, $CD5^-$, $CD56^-$, $CD7^+$, $CD19^-$, $CD34^-$, $CD14^-$, $CD11b^-$, $CD10^-$, $CD41b^-$, $CD41a^-$). Other markers were $CD11a^{low/-}$, $CD11b^+$, $CD18^{+/low}$, $CD29^+$, $CD44^+$, $CD49e^+$, $CD49d^+$, $CD54^{low}$, $CD56^{+/-}$, $CD62L^{low}$, $CD117^+$, HLA-DR^+ (Fig. 1), which was also the same as the BM MNCs used for the injection of NOG mice (data not shown).

Following serial passage in NOG mice, TRL-01 cells were detected in the BM within 1 month after injection, and in the spleen and mesenterium 1 month later but rarely found in other organs ($n = 5$; data not shown). The injected mice survived >4 months without cachexia.

Analysis of 20 metaphases revealed the presence of two clones in TRL-01 cells: 46,XX,t(11;19)(q23;p13.3), add(12)(p11.2)[4]/45,idem,der(2)t(2;15)(q35;q15),−15[16] (Fig. 2A). The occurrence of clonal evolution during the in vivo passage was suggested with the result of G-band analysis. The 46,idem,i(21)(q10) and 46,idem,add(21)(q22) detected at diagnosis were lost and a 45,idem,der(2) t(2;15)(q35;q15),−15 was generated in TRL-01. The *MLL*

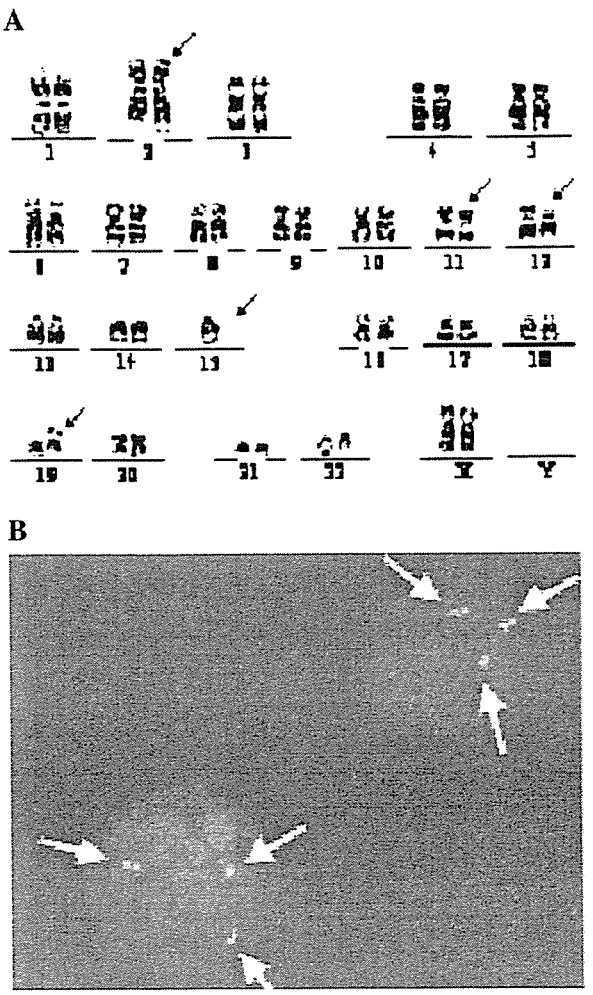

Fig. 2. Karyotypic and dual-color fluorescence in situ hybridization (DC-FISH) analyses. (A) Karyotype of TRL-01. Arrows indicate chromosomal alterations. (B) DC-FISH analyses were performed as described in the Materials and Methods section. Locus-specific probes for *MLL* gene breakpoint cluster region (bcr) labeled in SpectrumGreen and an ~190-kbp portion largely telomeric of the bcr labeled in SpectrumOrange were used. Cells with a fusion spot indicate a normal *MLL* allele (white arrows); split signals of green and orange are indicative of the *MLL* translocation (yellow arrows).

gene translocation was identified by DC-FISH analyses using a locus-specific probe for the *MLL* gene bcr labeled in SpectrumGreen and the telomeric bcr labeled in SpectrumOrange in the original AML cells and TRL-01 cells (Fig. 2B). This data suggested that the *MLL* gene, which is located at 11q23, was fused to a partner gene located at 19p13.

Because three kinds of fusion genes (*MLL-ENL*, *MLL-ELL*, and *MLL-MEN*) have been known in t(11;19)(q23;p13) [12,13,17], we amplified these fusion cDNAs by RT-PCR using appropriate primers; however, no bands were amplified (data not shown). We then applied the cDNA panhandle PCR method to obtain the fusion transcripts of *MLL*. Several PCR products were amplified in TRL-01 cells and the BM MNCs at diagnosis. The sequence of the PCR products revealed that exon 6 of the *MLL* gene (11q23) fused to exon 4 of the *ENL* gene (19p13.3), a breakpoint that has not been reported previously (Fig. 3A). The other cDNA panhandle PCR products had the wild-type *MLL* (data not shown). With the *MLL* primer 4 and *ENL* primer 1 (see Supplemental Data), a 438-bp PCR product was confirmed during the four

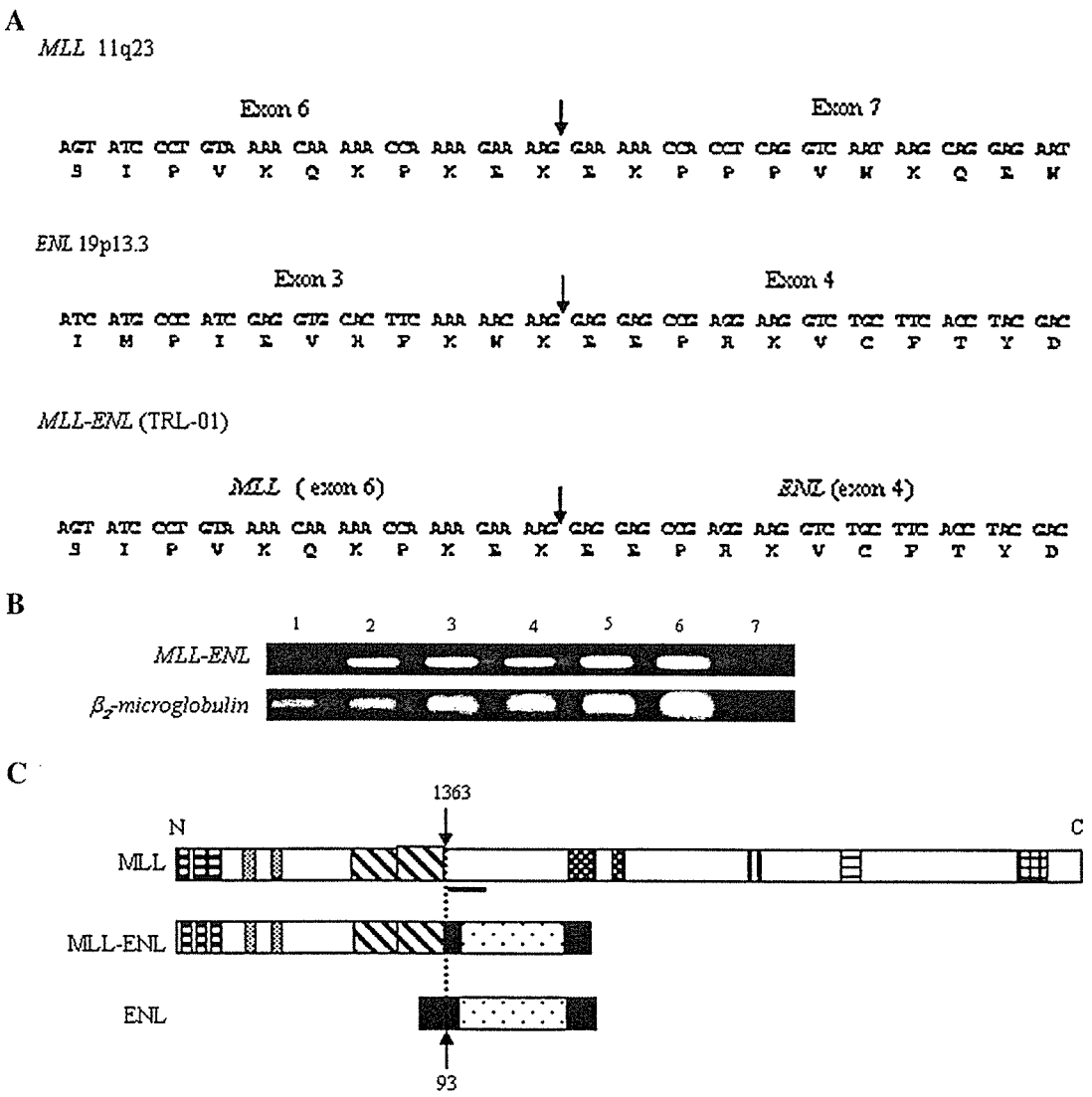

Fig. 3. Sequence of the cloned panhandle PCR product from TRL-01. (A) Normal sequence of *MLL* exon 6–exon 7, *ENL* exon 3–exon 4, and sequence of TRL-01. Arrows indicate the exon–exon boundaries. (B) RT-PCR of the *MLL-ENL* cDNA. Primers were *MLL* primer 4 and *ENL* primer 1, which gave PCR products at 438 bp. Lane 1, RS4;11; lane 2, BM MNC at diagnosis; lane 3, the spleen cells from NOG mouse in 1st passage; lane 4, the spleen cells from NOG mouse in 2nd passage; lane 5, the spleen cells from NOG mouse in 3rd passage; lane 6, the spleen cells from NOG mouse in 4th passage; lane 7, H_2O. As a positive control, primers for β_2-microglobulin were used. (C) Schematic representation of MLL, MLL-ENL, and ENL proteins: *Banding legend (left to right):* dark horizontal lines, AT hook; dotted white on gray, SNL1 and SNL2; slanted lines, repression domains (RD1 and RD2); closely dotted white on black, PHD zinc finger; vertical line, cleavage site; light horizontal lines, transactivation domain; and checkered, SET domain. The dark horizontal line below indicates the breakpoint cluster region of MLL. Solid black, ANC-1 homologous region; white, serine-proline rich region of ENL.

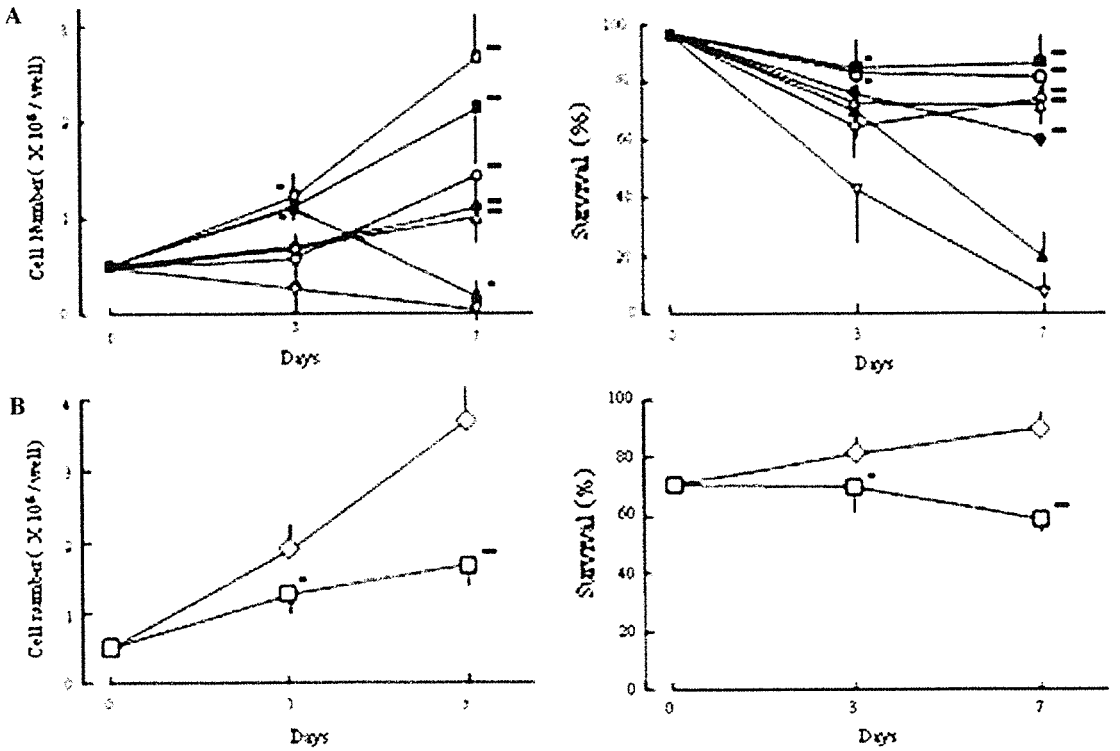

Fig. 4. TRL-01 required direct adhesion to specific stroma cells for growth. TRL-01 cells (1×10^5/mL, 5 mL) cultivated on MS-5 (open squares), HESS-5 (solid squares), OP-9 (open triangles up), COS-7 (solid circles), 293T (open circles), or NIH3T3 (solid triangles up) cells (5×10^3/mL), and no stroma cells (open triangles down) in 6-well plates for 7 days. (A) Data indicate cell number (left panel) and survival (%) (right panel). (B) Cultivation of TRL-01 (1×10^5/mL, 5 mL) on HESS-5 monolayer (5×10^3/mL) in 6-well plates with (open squares) or without (open diamonds) use of cell culture inserts for 7 days. Data indicate cell number (left panel) and survival (%) (right panel). **, $P<0.01$; *, $P<0.05$.

passages in the NOG mice (Fig. 3B). This result indicated that TRL-01 cells bearing t(11;19) stably maintained in the NOG mice environment.

We cultivated TRL-01 on various BM stroma cell lines to study which supported survival and growth of TRL-01 ex vivo. The best conditions were obtained in the culture with HESS-5 and MS-5 both of which are derived from mouse BM stroma cells ($n = 3$, $P < 0.01$; Fig. 4A). TRL-01 cells proliferated with a doubling time of 3–4 days, and the rate of cell survival remained >80%. COS-7, OP-9, and 293T cells partially stimulated the proliferation, with a doubling time of 5–7 days, whereas survival was moderately maintained. NIH3T3 cells did not support proliferation or survival (Fig. 4A). To study the requirement of direct adherence of TRL-01 to HESS-5, a membrane (BD cell culture insert) was inserted to prevent direct adherence between TRL-01 and HESS-5 but allow soluble factors to pass. The proliferation and survival of TRL-01 were significantly inhibited by the use of the cell culture insert ($n = 3$, $P < 0.01$; Fig. 4B). These results clearly indicate that TRL-01 required direct adherence to BM stroma cells for proliferation and survival.

To examine the effect of adherence to fibronectin on apoptosis, flow-cytometric analyses of TRL-01 cultivated on fibronectin-coated plates for 7 days were performed. A percentage of the apoptosis (lower-right fraction of two-color analyses using propidium iodide and annexin-V staining) were partly suppressed in the fibronectin-coated plates comparing to nontreated plates ($n = 3$, $P < 0.05$; Figs. 5A and 5B).

To determine the effect of growth factor on TRL-01 culture in a fibronectin-coated 6-well plate, 50 ng/mL of SCF, GM-CSF, G-SCF, TPO, or EPO was added. The cell numbers increased on treatment with GM-CSF ($n = 3$, $P < 0.01$), SCF ($n = 3$, $P < 0.01$), or G-CSF ($n = 3$, $P < 0.01$), whereas TPO and EPO had no effect on growth ($n = 3$; Fig. 6A). The survival of TRL-01 was slightly maintained under SCF ($n = 3$, $P < 0.05$) and G-CSF ($n = 3$, $P < 0.01$) treatment (Fig. 6B). No phenotypic or morphological changes were observed in TRL-01 cells treated with these factors ($n = 3$; data not shown).

To confirm the stroma dependency in vivo, we subcutaneously injected TRL-01 and HESS-5 into the dorsal regions of the NOG mice. Coinjection of TRL-01 and HESS-5 cells resulted in the tumors in the dorsal regions

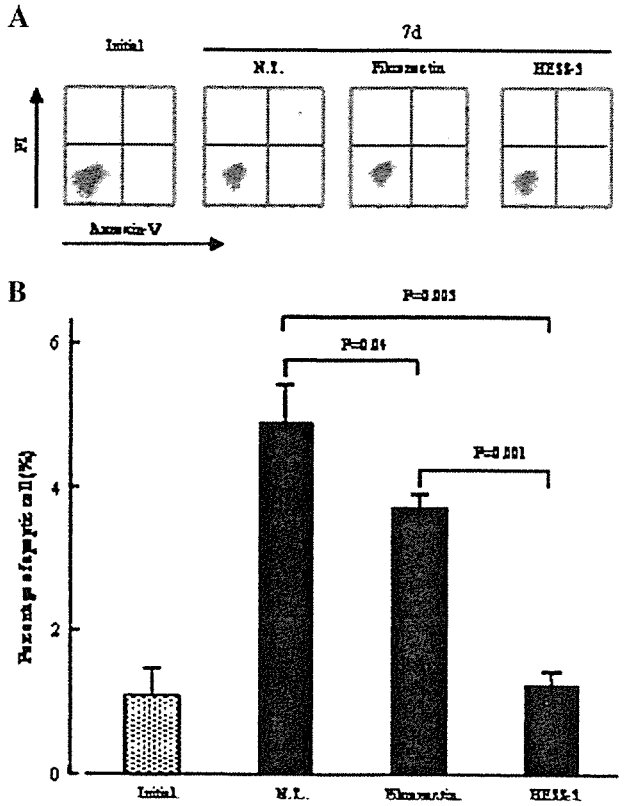

Fig. 5. Adhesion to the stroma cells inhibited apoptosis of TRL-01. (A) Flow-cytometric analyses of TRL-01 cells (1×10^5/mL, 5 mL), cultivated on fibronectin-coated 6-well plates or HESS-5 monolayer (5×10^3/mL) in 6-well plates for 7 days, with two-color propidium iodide and annexin-V staining. (B) Data indicate the percentage of the lower-right (apoptosis) fraction for 7 days cultivation of TRL-01. N.T., non-treated plate.

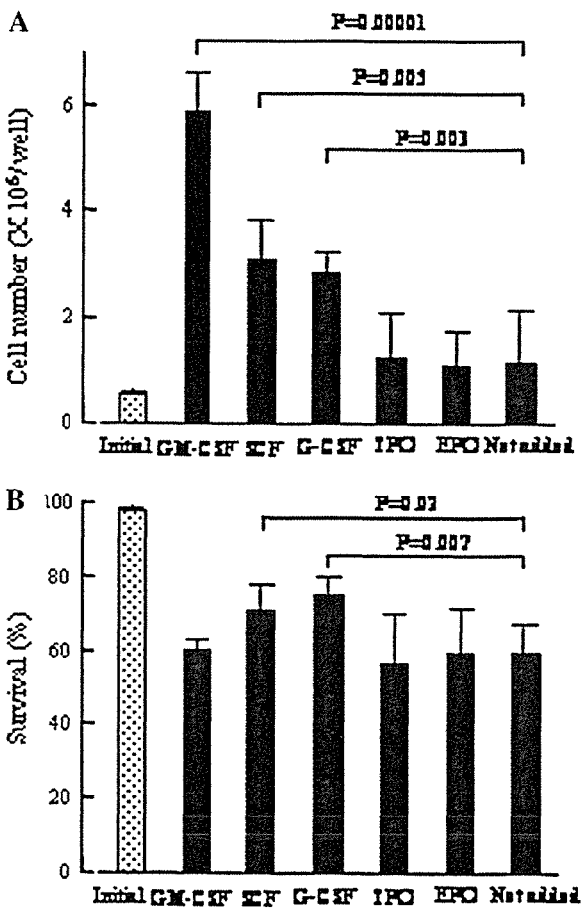

Fig. 6. Growth factors enhanced proliferation of TRL-01. TRL-01 (1×10^5/mL, 5 mL) cultivated on fibronectin-coated 6-well plates for 7 days with 50 ng/mL of growth factors. (A) Cell number. (B) Survival (%).

40 days after the injection ($n = 3$; Fig. 7A), whereas TRL-01 alone ($n = 3$) or HESS-5 alone ($n = 3$) did not form any tumors (Fig. 7A). In terms of pathology, the subcutaneous tumor was filled with myeloblastic cells ($n = 3$; Fig. 7B, plate 1) and was strongly stained with human CD45 immunostaining ($n = 3$; Fig. 7B, plate 2). Human $CD45^+$ cells were detected mainly in the BM and rarely found in other organs ($n = 3$; Fig. 7B, plates 3 and 4). From RT-PCR analysis, *MLL-ENL* expression was also confirmed in the subcutaneous tumor (Fig. 7C). These findings suggest that the proliferation and survival of TRL-01 depend on BM stroma cells in vivo as well as in vitro.

4. Discussion

One characteristic of TRL-01 is that it is an undifferentiated AML cell line with the *MLL-ENL* fusion gene. So far, several leukemia cell lines harboring *MLL-ENL* have been reported [11,18]. Their phenotypes are exclusively lymphoid, including pre-B ALL and pre-T ALL [19], although *MLL-ENL* is found in both myeloid and lymphoid lineages [20,21]. In most cases of *MLL-ENL*, generation of *MLL* exon 7 and *ENL* exon 2 chimeric transcripts was reported [11]. In the transcripts of TRL-01, exon 6 of the *MLL* gene was fused to exon 4 of the *ENL* gene. In both cases, an in-frame chimeric *MLL-ENL* is generated and major functional domains are the same (Fig. 3C).

Although the exact functional role of the MLL-ENL chimeric protein remains unclear, it has been suggested to be the upregulation of the transcription of *HOX9a* and *MEIS1*, which are associated with self-renewal and differentiation block [22]. It has recently been shown in a murine model that expression of *MLL-ENL* can convert a hematopoietic stem cell that has intrinsic self-renewal capacity, or even a committed hematopoietic progenitor cell that has no capacity for self-renewal, into a cell that has the properties of a leukemia stem cell [23]. Many investigators now think that a second hit such as a *FLT3* mutation would confer additional proliferative and survival advantages to these cells [24]. TRL-01, however, has neither surface expression nor